Computers and Mathematics with Applications 80 (2020) 2538–2562

Contents lists available at ScienceDirect

Computers and Mathematics with Applications

journal homepage: www.elsevier.com/locate/camwa

Isogeometric analysis with C^1 hierarchical functions on planar two-patch geometries

Cesare Bracco [a], Carlotta Giannelli [a], Mario Kapl [b,*], Rafael Vázquez [c,d]

[a] Dipartimento di Matematica e Informatica "U. Dini", Università degli Studi di Firenze, Florence, Italy
[b] Johann Radon Institute for Computational and Applied Mathematics, Austrian Academy of Sciences, Linz, Austria
[c] Institute of Mathematics, École Polytechnique Fédérale de Lausanne, Lausanne, Switzerland
[d] Istituto di Matematica Applicata e Tecnologie Informatiche 'E. Magenes' del CNR, Pavia, Italy

ARTICLE INFO

Article history:
Available online 11 April 2020

Keywords:
Isogeometric analysis
Geometric continuity
Two-patch domain
Hierarchical splines
Local refinement

ABSTRACT

Adaptive isogeometric methods for the solution of partial differential equations rely on the construction of locally refinable spline spaces. A simple and efficient way to obtain these spaces is to apply the multi-level construction of hierarchical splines, that can be used on single-patch domains or in multi-patch domains with C^0 continuity across the patch interfaces. Due to the benefits of higher continuity in isogeometric methods, recent works investigated the construction of spline spaces with global C^1 continuity on two or more patches. In this paper, we show how these approaches can be combined with the hierarchical construction to obtain global C^1 continuous hierarchical splines on two-patch domains. A selection of numerical examples is presented to highlight the features and effectivity of the construction.

© 2020 Elsevier Ltd. All rights reserved.

1. Introduction

Isogeometric Analysis (IgA) is a framework for numerically solving partial differential equations (PDEs), see [1–3], by using the same (spline) function space for describing the geometry (i.e. the computational domain) and for representing the solution of the considered PDE. One of the strong points of IgA compared to finite elements is the possibility to easily construct C^1 spline spaces, and to use them for solving fourth order PDEs by applying a Galerkin discretization to their variational formulation. Examples of fourth order problems with practical relevance (in the frame of IgA) are e.g. the biharmonic equation [4–6], the Kirchhoff–Love shells [7–10] and the Cahn–Hilliard equation [11–13].

Adaptive isogeometric methods can be developed by combining the IgA framework with spline spaces that have local refinement capabilities. Hierarchical B-splines [14,15] and truncated hierarchical B-splines [16,17] are probably the adaptive spline technologies that have been studied more in detail in the adaptive IgA framework [18–20]. Their multi-level structure makes them easy to implement, with the evaluation of basis functions obtained via a recursive use of two-level relation due to nestedness of levels [21–23]. Hierarchical B-splines have been successfully applied for the adaptive discretization of fourth order PDEs, and in particular for phase-field models used in the simulation of brittle fracture [23,24] or tumor growth [25].

While the construction of C^1 spaces is trivial in a single-patch domain, either using B-splines or hierarchical B-splines, the same is not true for general multi-patch domains. The construction of C^1 spline spaces over multi-patch domains

* Corresponding author.
E-mail addresses: cesare.bracco@unifi.it (C. Bracco), carlotta.giannelli@unifi.it (C. Giannelli), mario.kapl@ricam.oeaw.ac.at (M. Kapl), rafael.vazquez@epfl.ch (R. Vázquez).

https://doi.org/10.1016/j.camwa.2020.03.018
0898-1221/© 2020 Elsevier Ltd. All rights reserved.

List of symbols

Spline space

p	Spline degree, $p \geq 3$
r	Spline regularity, $1 \leq r \leq p-2$
Ξ_p^r	Open knot vector
τ_i	Internal breakpoints of knot vector Ξ_p^r
T	Ordered set of internal breakpoints τ_i
k	Number of different internal breakpoints of knot vector Ξ_p^r
$\mathbb{S}_p^r$	Univariate spline space of degree p and regularity r on $[0, 1]$ over knot vector Ξ_p^r
$\mathbb{S}_p^{r+1}$, $\mathbb{S}_{p-1}^r$	Univariate spline spaces of higher regularity and lower degree, respectively, defined from same internal breakpoints as $\mathbb{S}_p^r$
$N_{i,p}^r$, $N_{i,p}^{r+1}$, $N_{i,p-1}^r$	B-splines of spline spaces $\mathbb{S}_p^r$, $\mathbb{S}_p^{r+1}$ and $\mathbb{S}_{p-1}^r$, respectively
n, n_0, n_1	Dimensions of spline spaces $\mathbb{S}_p^r$, $\mathbb{S}_p^{r+1}$ and $\mathbb{S}_{p-1}^r$, respectively
$\mathbf{I}$, $\mathbf{I}_0$, $\mathbf{I}_1$	Index sets of B-splines $N_{i,p}^r$, $N_{i,p}^{r+1}$ and $N_{i,p-1}^r$, respectively
$\mathbf{J}_{0,i}$, $\mathbf{J}_{1,i}$	Index subsets of $\mathbf{I}$ related to B-splines $N_{i,p}^{r+1}$ and $N_{i,p-1}^r$, for $i \in \mathbf{I}_0$ and $i \in \mathbf{I}_1$, respectively
ζ_m	Greville abscissae of spline space $\mathbb{S}_p^r$, $m \in \mathbf{I}$
$\mathbf{N}_0$, $\mathbf{N}_1$, $\mathbf{N}_2$	Vectors of tensor-product B-splines $N_{i,p}^r N_{j,p}^r$

Geometry

(S)	Upper index referring to specific patch, $S \in \{L, R\}$
$\Omega^{(S)}$	Quadrilateral patch
Ω	Two-patch domain $\Omega = \Omega^{(L)} \cup \Omega^{(R)}$
Γ	Common interface of two-patch domain Ω
$\mathbf{F}^{(S)}$	Geometry mapping of patch $\Omega^{(S)}$
$\mathbf{F}$	Two patch geometry $\mathbf{F} = (\mathbf{F}^{(L)}, \mathbf{F}^{(R)})$
$\mathbf{F}_0$	Parameterization of interface Γ
$\mathbf{d}$	Specific transversal vector to Γ
ξ_1, ξ_2	Parameter directions of geometry mappings
$\mathbf{c}_{i,j}^{(S)}$	Spline control points of geometry mapping $\mathbf{F}^{(S)}$
$\alpha^{(S)}$, $\beta^{(S)}$, β	Gluing functions of two-patch geometry $\mathbf{F}$
γ	Scalar function, $\gamma \neq 0$

C^1 isogeometric space

$\mathbb{V}$	Space of C^1 isogeometric spline functions on Ω
$\mathbb{W}$	Subspace of $\mathbb{V}$
Φ	Basis of $\mathbb{W}$
$\Phi_{\Omega^{(S)}}$, Φ_{Γ_0}, Φ_{Γ_1}	Parts of basis Φ, $\Phi = \Phi_{\Omega^{(L)}} \cup \Phi_{\Omega^{(R)}} \cup \Phi_{\Gamma_0} \cup \Phi_{\Gamma_1}$
$\phi_{i,j}^{\Omega^{(S)}}$	Basis functions of $\Phi_{\Omega^{(S)}}$, $i \in \mathbf{I} \setminus \{0, 1\}$, $j \in \mathbf{I}$
$\phi_i^{\Gamma_0}$	Basis functions of Φ_{Γ_0}, $i \in \mathbf{I}_0$
$\phi_i^{\Gamma_1}$	Basis functions of Φ_{Γ_1}, $i \in \mathbf{I}_1$
$\widehat{\boldsymbol{\phi}}_{\Gamma_0}^{(S)}$, $\widehat{\boldsymbol{\phi}}_{\Gamma_1}^{(S)}$, $\widehat{\boldsymbol{\phi}}_{\Omega^{(S)}}^{(S)}$	Vectors of spline functions $\phi_i^{\Gamma_0} \circ \mathbf{F}^{(S)}$, $\phi_i^{\Gamma_1} \circ \mathbf{F}^{(S)}$ and $\phi_{i,j}^{\Omega^{(S)}} \circ \mathbf{F}^{(S)}$, respectively
$\widehat{B}$, $\widetilde{B}^{(S)}$, $\overline{B}^{(S)}$	Transformation matrices
$\widehat{b}_{i,j}$, $\widetilde{b}_{i,j}^{(S)}$, $\overline{b}_{i,j}^{(S)}$	Entries of matrices $\widehat{B}$, $\widetilde{B}^{(S)}$ and $\overline{B}^{(S)}$, respectively
$B^{(S)}$	Block matrix assembled by the matrices $\widehat{B}$, $\widetilde{B}^{(S)}$, $\overline{B}^{(S)}$ and the identity matrix $I_{n(n-2)}$

Hierarchical space

ℓ	Upper index referring to specific level
$\Lambda_p^{r,\ell+1}$, $\Lambda_p^{r+1,\ell+1}$, $\Lambda_{p-1}^{r,\ell+1}$	Refinement matrices for B-splines $N_{i,p}^{r,\ell}$, $N_{i,p}^{r+1,\ell}$ and $N_{i,p-1}^{r,\ell}$, respectively
$\lambda_{i,j}^{\ell+1}$	Entries of refinement matrix $\Lambda_p^{r,\ell+1}$
$\Theta_{ij}^{\ell+1}$	Block matrices of refinement mask $\Lambda_p^{r,\ell+1} \otimes \Lambda_p^{r,\ell+1}$, $0 \leq i \leq j \leq 2$

$\mathbb{W}_H$	C^1 hierarchical isogeometric spline space
$\mathcal{W}$	Basis of $\mathbb{W}_H$

Most notations in the paragraphs "Spline space" and "C^1 isogeometric space" can be directly extended to the hierarchical setting by adding the upper index ℓ to refer to the considered level.

is based on the concept of geometric continuity [26,27], which is a well-known framework in computer-aided design (CAD) for the design of smooth multi-patch surfaces. The core idea is to employ the fact that an isogeometric function is C^1-smooth if and only if the associated multi-patch graph surface is G^1-smooth [28], i.e., it is geometrically continuous of order 1.

In the last few years there has been an increasing effort to provide methods for the construction of globally C^1 isogeometric spline spaces over general multi-patch domains. Before giving a short overview of these existing techniques, we first point to the approach [29], where a smooth multi-patch spline space has been generated, which is C^1 (or even C^{p-1}) across all interfaces but just C^0 in the vicinity of an extraordinary vertex, and which has been extended to a hierarchical setting, too.

The existing methods for the design of globally C^1 isogeometric spline spaces for planar multi-patch domains can be roughly classified into two groups depending on the used parameterization for the domain. The first approach relies on a multi-patch parameterization which is C^1-smooth everywhere except in the neighborhood of extraordinary vertices (i.e. vertices with valencies different to four), where the parameterization is singular, see e.g. [30–32], or consists of a special construction, see e.g. [33–35]. The methods [30–32] use a singular parameterization with patches in the vicinity of an extraordinary vertex, which belong to a specific class of degenerate (Bézier) patches introduced in [36], and that allow, despite having singularities, the design of globally C^1 isogeometric spaces. The techniques [33–35] are based on G^1 multi-patch surface constructions, where the obtained surface in the neighborhood of an extraordinary vertex consists of patches of slightly higher degree [33,35] and is generated by means of a particular subdivision scheme [34]. As a special case of the first approach can be seen the constructions in [37,38], that employ a polar framework to generate C^1 spline spaces.

The second approach, on which we will focus, uses a particular class of regular C^0 multi-patch parameterizations, called analysis-suitable G^1 multi-patch parameterization [4]. The class of analysis-suitable G^1 multi-patch geometries characterizes the regular C^0 multi-patch parameterizations that allow the design of C^1 isogeometric spline spaces with optimal approximation properties, see [4,39], and includes for instance the subclass of bilinear multi-patch parameterizations [5,40,41]. An algorithm for the construction of analysis-suitable G^1 parameterizations for complex multi-patch domains was presented in [39]. The main idea of this approach is to analyze the entire space of C^1 isogeometric functions over the given multi-patch geometry to generate a basis of this space or of a suitable subspace. While the methods in [5,40,41] are mainly restricted to (mapped) bilinear multi-patch parameterizations, the techniques [42–46] can also deal with more general multi-patch geometries. An alternative but related approach comprises the constructions [47,48] for general C^0 multi-patch parameterizations, which increase the degree of the constructed spline functions in the neighborhood of the common interfaces to obtain C^1 isogeometric spaces with good approximation properties.

In this work, we extend for the case of two-patch domains the second approach from above to the construction of *hierarchical* C^1 isogeometric spaces on analysis-suitable G^1 geometries, using the abstract framework for the definition of hierarchical splines detailed in [17]. We show that the basis functions of the considered C^1 space on analysis-suitable G^1 two-patch parameterizations, which is a subspace of the space [43] inspired by [45], satisfy the required properties given in [17], and in particular that the basis functions are locally linearly independent (see Section 3.1 for details). Note that in case of a multi-patch domain, the general framework for the construction of hierarchical splines [17] cannot be used anymore, since the appropriate C^1 basis functions [45] can be locally linearly dependent. Therefore, the development of another approach as [17] would be needed for the multi-patch case, which is beyond the scope of this paper.

For the construction of the hierarchical C^1 spline spaces on analysis-suitable G^1 two-patch geometries, we also explore the explicit expression for the relation between C^1 basis functions of two consecutive levels, expressing coarse basis functions as linear combinations of fine basis functions. This relation is exploited for the implementation of hierarchical splines as in [22,23]. A series of numerical tests are presented, that are run with the help of the Matlab/Octave code GeoPDEs [22,49].

The remainder of the paper is organized as follows. Section 2 recalls the concept of analysis-suitable G^1 two-patch geometries and presents the used C^1 isogeometric spline space over this class of parameterizations. In Section 3, we develop the (theoretical) framework to employ this space to construct C^1 hierarchical isogeometric spline spaces, which includes the verification of the nested nature of this kind of spaces, as well as the proof of the local linear independence of the one-level basis functions. Additional details of the C^1 hierarchical construction, such as the refinement masks of the basis functions for the different levels, are discussed in Section 4 with focus on implementation aspects. The generated hierarchical spaces are then used in Section 5 to numerically solve the laplacian and bilaplacian equations on two-patch geometries, where the numerical results demonstrate the potential of our C^1 hierarchical construction for applications in IgA. Finally, the concluding remarks can be found in Section 6. The construction of the non-trivial analysis-suitable G^1 two-patch parameterization used in some of the numerical examples is described in detail in Appendix. For easiness of reading, we include a list of symbols with the main notation used in this work.

2. C^1 Isogeometric spaces on two-patch geometries

In this section, we introduce the specific class of two-patch geometries and the C^1 isogeometric spaces which will be used throughout the paper.

2.1. Analysis-suitable G^1 two-patch geometries

We present a particular class of planar two-patch geometries, called analysis-suitable G^1 two-patch geometries, which was introduced in [4]. This class is of importance since it comprises exactly those two-patch geometries which are suitable for the construction of C^1 isogeometric spaces with optimal approximation properties, see [4,39]. The most prominent member is the subclass of bilinear two-patch parameterizations, but it was demonstrated in [39] that the class is much wider and allows the design of generic planar two-patch domains.

Let $k, p, r \in \mathbb{N}$ with degree $p \geq 3$ and regularity $1 \leq r \leq p-2$. Let us also introduce the ordered set of internal breakpoints $T = \{\tau_1, \tau_2, \ldots, \tau_k\}$, with $0 < \tau_i < \tau_{i+1} < 1$ for all $1 \leq i \leq k$. We denote by $\mathbb{S}_p^r$ the univariate spline space in $[0, 1]$ with respect to the open knot vector

$$\Xi_p^r = \{ \underbrace{0, \ldots, 0}_{(p+1)-\text{times}}, \underbrace{\tau_1, \ldots, \tau_1}_{(p-r)-\text{times}}, \underbrace{\tau_2, \ldots, \tau_2}_{(p-r)-\text{times}}, \ldots, \underbrace{\tau_k, \ldots, \tau_k}_{(p-r)-\text{times}}, \underbrace{1, \ldots, 1}_{(p+1)-\text{times}} \}, \tag{1}$$

and let $N_{i,p}^r$, $i \in \mathbf{I} = \{0, \ldots, p + k(p-r)\}$, be the associated B-splines. Note that the parameter r specifies the resulting C^r-continuity of the spline space $\mathbb{S}_p^r$. We will also make use of the subspaces of higher regularity and lower degree, respectively $\mathbb{S}_p^{r+1}$ and $\mathbb{S}_{p-1}^r$, defined from the same internal breakpoints, and we will use an analogous notation for their basis functions. Furthermore, we denote by n, n_0 and n_1 the dimensions of the spline spaces $\mathbb{S}_p^r$, $\mathbb{S}_p^{r+1}$ and $\mathbb{S}_{p-1}^r$, respectively, which are given by

$$n = p + 1 + k(p-r), \quad n_0 = p + 1 + k(p-r-1) \text{ and } n_1 = p + k(p-r-1),$$

and, analogously to $\mathbf{I}$, we introduce the index sets

$$\mathbf{I}_0 = \{0, \ldots, n_0 - 1\}, \qquad \mathbf{I}_1 = \{0, \ldots, n_1 - 1\},$$

corresponding to basis functions in $\mathbb{S}_p^{r+1}$ and $\mathbb{S}_{p-1}^r$, respectively.

Let $\mathbf{F}^{(L)}, \mathbf{F}^{(R)} \in (\mathbb{S}_p^r \otimes \mathbb{S}_p^r)^2$ be two regular spline parameterizations, whose images $\mathbf{F}^{(L)}([0,1]^2)$ and $\mathbf{F}^{(R)}([0,1]^2)$ define the two quadrilateral patches $\Omega^{(L)}$ and $\Omega^{(R)}$ via $\mathbf{F}^{(S)}([0,1]^2) = \Omega^{(S)}$, $S \in \{L, R\}$. The regular, bijective mapping $\mathbf{F}^{(S)} : [0,1]^2 \to \Omega^{(S)}$, $S \in \{L, R\}$, is called *geometry mapping*, and possesses a spline representation

$$\mathbf{F}^{(S)}(\xi_1, \xi_2) = \sum_{i \in \mathbf{I}} \sum_{j \in \mathbf{I}} \mathbf{c}_{i,j}^{(S)} N_{i,p}^r(\xi_1) N_{j,p}^r(\xi_2), \quad \mathbf{c}_{i,j}^{(S)} \in \mathbb{R}^2.$$

We assume that the two patches $\Omega^{(L)}$ and $\Omega^{(R)}$ form a planar two-patch domain $\Omega = \Omega^{(L)} \cup \Omega^{(R)}$, which share one whole edge as common interface $\Gamma = \Omega^{(L)} \cap \Omega^{(R)}$. In addition, and without loss of generality, we assume that the common interface Γ is parameterized by $\mathbf{F}_0 : [0,1] \to \Gamma$ via

$$\mathbf{F}_0(\xi_2) = \mathbf{F}^{(L)}(0, \xi_2) = \mathbf{F}^{(R)}(0, \xi_2), \quad \xi_2 \in [0,1],$$

and denote by $\mathbf{F}$ the two-patch parameterization (also called *two-patch geometry*) consisting of the two spline parameterizations $\mathbf{F}^{(L)}$ and $\mathbf{F}^{(R)}$.

Remark 1. For simplicity, we have restricted ourselves to a univariate spline space $\mathbb{S}_p^r$ with the same knot multiplicity for all inner knots. Instead, a univariate spline space with different inner knot multiplicities can be used, as long as the multiplicity of each inner knot is at least 2 and at most $p-1$. Note that the subspaces $\mathbb{S}_p^{r+1}$ and $\mathbb{S}_{p-1}^r$ should also be replaced by suitable spline spaces of regularity increased by one at each inner knot, and degree reduced by one, respectively. Furthermore, it is also possible to use different univariate spline spaces for both Cartesian directions and for both geometry mappings, with the requirement that both patches must have the same univariate spline space in ξ_2-direction.

The two geometry mappings $\mathbf{F}^{(L)}$ and $\mathbf{F}^{(R)}$ uniquely determine up to a common function $\gamma : [0,1] \to \mathbb{R}$ (with $\gamma \neq 0$), the functions $\alpha^{(L)}, \alpha^{(R)}, \beta : [0,1] \to \mathbb{R}$ given by

$$\alpha^{(S)}(\xi_2) = \gamma(\xi_2) \det\left(\partial_1 \mathbf{F}^{(S)}(0, \xi_2), \partial_2 \mathbf{F}^{(S)}(0, \xi_2)\right), \quad S \in \{L, R\},$$

and

$$\beta(\xi_2) = \gamma(\xi_2) \det\left(\partial_1 \mathbf{F}^{(L)}(0, \xi_2), \partial_1 \mathbf{F}^{(R)}(0, \xi_2)\right),$$

satisfying for $\xi_2 \in [0,1]$

$$\alpha^{(L)}(\xi_2)\alpha^{(R)}(\xi_2) < 0 \tag{2}$$

and

$$\alpha^{(R)}\partial_1\mathbf{F}^{(L)}(0,\xi_2)-\alpha^{(L)}(\xi_2)\partial_1\mathbf{F}^{(R)}(0,\xi_2)+\beta(\xi_2)\partial_2\mathbf{F}^{(L)}(0,\xi_2)=\mathbf{0}. \tag{3}$$

In addition, there exist non-unique functions $\beta^{(L)}$ and $\beta^{(R)}:[0,1]\to\mathbb{R}$ such that

$$\beta(\xi_2)=\alpha^{(L)}(\xi_2)\beta^{(R)}(\xi_2)-\alpha^{(R)}(\xi_2)\beta^{(L)}(\xi_2), \tag{4}$$

see e.g. [4,27]. The two-patch geometry $\mathbf{F}$ is called *analysis-suitable* G^1 if there exist linear polynomial functions $\alpha^{(S)}$, $\beta^{(S)}$, $S\in\{L,R\}$ with $\alpha^{(L)}$ and $\alpha^{(R)}$ relatively prime[1] such that Eqs. (2)–(4) are satisfied for $\xi_2\in[0,1]$, see [4,43]. Note that requiring that $\alpha^{(L)}$ and $\alpha^{(R)}$ are relatively prime is not restrictive: if $\alpha^{(L)}$ and $\alpha^{(R)}$ share a common factor, it is a factor of γ too, thus $\alpha^{(L)}$ and $\alpha^{(R)}$ can be made relatively prime by dividing by such a factor. Note that $\alpha^{(L)}$ and $\alpha^{(R)}$ being linear is also not restrictive, since the conditions are valid for non polynomial parameterizations, such as splines or NURBS, see [4,39].

In the following, we will only consider planar two-patch domains Ω which are described by analysis-suitable G^1 two-patch geometries $\mathbf{F}$. Furthermore, we select uniquely determined linear polynomial functions $\alpha^{(S)}$ and $\beta^{(S)}$, $S\in\{L,R\}$, by minimizing the terms

$$\|\alpha^{(L)}+1\|^2_{L^2([0,1])}+\|\alpha^{(R)}-1\|^2_{L^2([0,1])}$$

and

$$\|\beta^{(L)}\|^2_{L^2([0,1])}+\|\beta^{(R)}\|^2_{L^2([0,1])}.$$

The chosen linear polynomials $\alpha^{(S)}$ and $\beta^{(S)}$, $S\in\{L,R\}$, will ensure later a more uniform scaling of the basis functions, and are in case of parametric continuity, i.e. $\beta=0$ and $\alpha^{(L)}=-\alpha^{(R)}$ just the simple functions $\beta^{(L)}=\beta^{(R)}=0$ and $\alpha^{(L)}=-1$, $\alpha^{(R)}=1$, see [45].

2.2. The C^1 isogeometric space $\mathbb{V}$ and the subspace $\mathbb{W}$

We recall the concept of C^1 isogeometric spaces over analysis-suitable G^1 two-patch geometries studied in [4,43], and especially focus on a specific subspace of the entire space of C^1 isogeometric functions.

The space $\mathbb{V}$ of C^1 isogeometric spline functions on Ω (with respect to the two-patch geometry $\mathbf{F}$ and spline space $\mathbb{S}^r_p$) is given by

$$\mathbb{V}=\{\phi\in C^1(\Omega)\ :\ \phi\circ\mathbf{F}^{(S)}\in\mathbb{S}^r_p\otimes\mathbb{S}^r_p,\ S\in\{L,R\}\}. \tag{5}$$

A function $\phi:\Omega\to\mathbb{R}$ belongs to the space $\mathbb{V}$ if and only if the functions $f^{(S)}=\phi\circ\mathbf{F}^{(S)}$, $S\in\{L,R\}$, satisfy that

$$f^{(S)}\in\mathbb{S}^r_p\otimes\mathbb{S}^r_p,\quad S\in\{L,R\}, \tag{6}$$

$$f^{(L)}(0,\xi_2)=f^{(R)}(0,\xi_2),\quad \xi_2\in[0,1], \tag{7}$$

and

$$\alpha^{(R)}(\xi_2)\partial_1f^{(L)}(0,\xi_2)-\alpha^{(L)}(\xi_2)\partial_1f^{(R)}(0,\xi_2)+\beta(\xi_2)\partial_2f^{(L)}(0,\xi_2)=0,\quad \xi_2\in[0,1],$$

where the last equation is due to (4) further equivalent to

$$\frac{\partial_1f^{(L)}(0,\xi_2)-\beta^{(L)}(\xi_2)\partial_2f^{(L)}(0,\xi_2)}{\alpha^{(L)}(\xi_2)}=\frac{\partial_1f^{(R)}(0,\xi_2)-\beta^{(R)}(\xi_2)\partial_2f^{(R)}(0,\xi_2)}{\alpha^{(R)}(\xi_2)},\quad \xi_2\in[0,1], \tag{8}$$

see e.g. [4,28,41]. Therefore, the space $\mathbb{V}$ can be also described as

$$\mathbb{V}=\{\phi:\Omega\to\mathbb{R}\ :\ f^{(S)}=\phi\circ\mathbf{F}^{(S)},S\in\{L,R\},\ \text{fulfill Eqs. (6)–(8)}\}. \tag{9}$$

Note that the equally valued terms in (8) represent a specific directional derivative of ϕ across the interface Γ. In fact, recalling that $f^{(S)}=\phi\circ\mathbf{F}^{(S)}$ for $S\in\{L,R\}$, we have

$$\nabla\phi\cdot(\mathbf{d}\circ\mathbf{F}_0(\xi_2))=\nabla\phi\cdot(\mathbf{d}^{(S)}\circ\mathbf{F}_0(\xi_2))=\frac{\partial_1f^{(S)}(0,\xi_2)-\beta^{(S)}(\xi_2)\partial_2f^{(S)}(0,\xi_2)}{\alpha^{(S)}(\xi_2)},\quad \xi_2\in[0,1], \tag{10}$$

where $\mathbf{d}$ is a transversal vector to Γ given by $\mathbf{d}=\mathbf{d}^{(L)}=\mathbf{d}^{(R)}$ with $\mathbf{d}^{(S)}\circ\mathbf{F}_0(\xi_2)=(\partial_1\mathbf{F}^{(S)}(0,\xi_2),\partial_2\mathbf{F}^{(S)}(0,\xi_2))(1,-\beta^{(S)}(\xi_2))^T\frac{1}{\alpha^{(S)}(\xi_2)}$, $S\in\{L,R\}$, see [4,43].

The structure and the dimension of the space $\mathbb{V}$ heavily depends on the functions $\alpha^{(L)}$, $\alpha^{(R)}$ and β, and was fully analyzed in [43] by computing a basis and its dimension for all possible configurations. Below, we restrict ourselves to a simpler

[1] Two polynomials are relatively prime if their greatest common divisor has degree zero.

subspace $\mathbb{W}$ (motivated by [45]), which preserves the approximation properties of $\mathbb{V}$, and whose dimension is independent of the functions $\alpha^{(L)}$, $\alpha^{(R)}$ and β.

The C^1 isogeometric space $\mathbb{W}$ is defined as

$$\mathbb{W} = \operatorname{span} \Phi, \qquad \Phi = \Phi_{\Omega^{(L)}} \cup \Phi_{\Omega^{(R)}} \cup \Phi_{\Gamma_0} \cup \Phi_{\Gamma_1},$$

with

$$\Phi_{\Omega^{(S)}} = \left\{ \phi_{i,j}^{\Omega^{(S)}} \ : \ i \in \mathbf{I} \setminus \{0, 1\};\ j \in \mathbf{I} \right\}, \qquad S \in \{L, R\}, \tag{11}$$

$$\Phi_{\Gamma_0} = \left\{ \phi_i^{\Gamma_0} \ : \ i \in \mathbf{I}_0 \right\}, \qquad \Phi_{\Gamma_1} = \left\{ \phi_i^{\Gamma_1} \ : \ i \in \mathbf{I}_1 \right\}, \tag{12}$$

where the functions $\phi_{i,j}^{\Omega^{(S')}}$, $\phi_i^{\Gamma_0}$ and $\phi_i^{\Gamma_1}$ are defined via

$$\left(\phi_{i,j}^{\Omega^{(S')}} \circ \mathbf{F}^{(S)}\right)(\xi_1, \xi_2) = \begin{cases} N_{i,p}^r(\xi_1) N_{j,p}^r(\xi_2) & \text{if } S = S', \\ 0 & \text{otherwise,} \end{cases} \qquad i \in \mathbf{I} \setminus \{0, 1\};\ j \in \mathbf{I};\ S, S' \in \{L, R\}, \tag{13}$$

$$\left(\phi_i^{\Gamma_0} \circ \mathbf{F}^{(S)}\right)(\xi_1, \xi_2) = N_{i,p}^{r+1}(\xi_2)\left(N_{0,p}^r(\xi_1) + N_{1,p}^r(\xi_1)\right) + \beta^{(S)}(\xi_2)\left(N_{i,p}^{r+1}\right)'(\xi_2)\frac{\tau_1}{p} N_{1,p}^r(\xi_1), \quad i \in \mathbf{I}_0;\ S \in \{L, R\}, \tag{14}$$

and

$$\left(\phi_i^{\Gamma_1} \circ \mathbf{F}^{(S)}\right)(\xi_1, \xi_2) = \alpha^{(S)}(\xi_2) N_{i,p-1}^r(\xi_2) N_{1,p}^r(\xi_1), \quad i \in \mathbf{I}_1;\ S \in \{L, R\}. \tag{15}$$

The construction of the functions $\phi_{i,j}^{\Omega^{(S')}}$, $\phi_i^{\Gamma_0}$ and $\phi_i^{\Gamma_1}$ guarantees that they are linearly independent and therefore form a basis of the space $\mathbb{W}$. In addition, the functions fulfill equations (6)–(8) which implies that they are C^1-smooth on Ω, and hence $\mathbb{W} \subseteq \mathbb{V}$. When the two spaces $\mathbb{W}$ and $\mathbb{V}$ are equal, see [43] for details, the selection of the linear polynomial functions $\beta^{(S)}$, $S \in \{L, R\}$, changes the basis functions, but does not affect the subspace $\mathbb{W}$. In the case $\mathbb{W} \subsetneq \mathbb{V}$, the space $\mathbb{W}$ can vary for different choices of $\beta^{(S)}$. Since any selection of the functions $\beta^{(S)}$ will maintain the optimal approximation properties of $\mathbb{W}$, by the unique selection of $\beta^{(S)}$ described in Section 2.1 we uniquely determine the space $\mathbb{W}$.

The basis functions $\phi_{i,j}^{\Omega^{(S')}}$ are standard tensor-product B-splines whose support is included in one of the two patches, while the functions $\phi_i^{\Gamma_0}$ and $\phi_i^{\Gamma_1}$ are combinations of standard B-splines and their support crosses the interface Γ (see Fig. 1 for an example).

Moreover, the traces and specific directional derivatives (10) of the functions $\phi_i^{\Gamma_0}$ and $\phi_i^{\Gamma_1}$ at the interface Γ are equal to

$$\phi_i^{\Gamma_0} \circ \mathbf{F}_0(\xi_2) = N_{i,p}^{r+1}(\xi_2), \quad \phi_i^{\Gamma_1} \circ \mathbf{F}_0(\xi_2) = 0,$$

and

$$\nabla \phi_i^{\Gamma_0} \cdot (\mathbf{d} \circ \mathbf{F}_0(\xi_2)) = 0, \quad \nabla \phi_i^{\Gamma_1} \cdot (\mathbf{d} \circ \mathbf{F}_0(\xi_2)) = N_{i,p-1}^r(\xi_2).$$

Therefore, the C^1 isogeometric space $\mathbb{W}$ can be also characterized as

$$\mathbb{W} = \{\phi \in \mathbb{V} \ : \ \phi \circ \mathbf{F}_0(\xi_2) \in \mathbb{S}_p^{r+1} \text{ and } \nabla \phi \cdot (\mathbf{d} \circ \mathbf{F}_0(\xi_2)) \in \mathbb{S}_{p-1}^r\}. \tag{16}$$

In particular, this means that not only (7) and (8) are fulfilled, but that the terms in those equations respectively belong to the spline spaces $\mathbb{S}_p^{r+1}$ and $\mathbb{S}_{p-1}^r$.

3. C^1 Hierarchical isogeometric spaces on two-patch geometries

This section introduces an abstract framework for the construction of the hierarchical spline basis, that is defined in terms of a multilevel approach applied to an underlying sequence of spline bases that are *locally linearly independent* and characterized by *local and compact supports*. The C^1 hierarchical isogeometric spaces on two-patch geometries are then defined by applying the hierarchical construction to the C^1 isogeometric functions described in the previous section. Particular attention is devoted to the proof of local linear independence of the basis functions, cf. Section 3.2, and to the refinement mask that explicitly identifies a two-scale relation between hierarchical functions of two consecutive levels, cf. Section 4.2. Note that, even if the hierarchical framework can be applied with different refinement strategies between consecutive refinement levels, we here focus on dyadic refinement, the standard choice in most application contexts. In the following the refinement level ℓ is denoted as a superscript associated to the corresponding symbol.

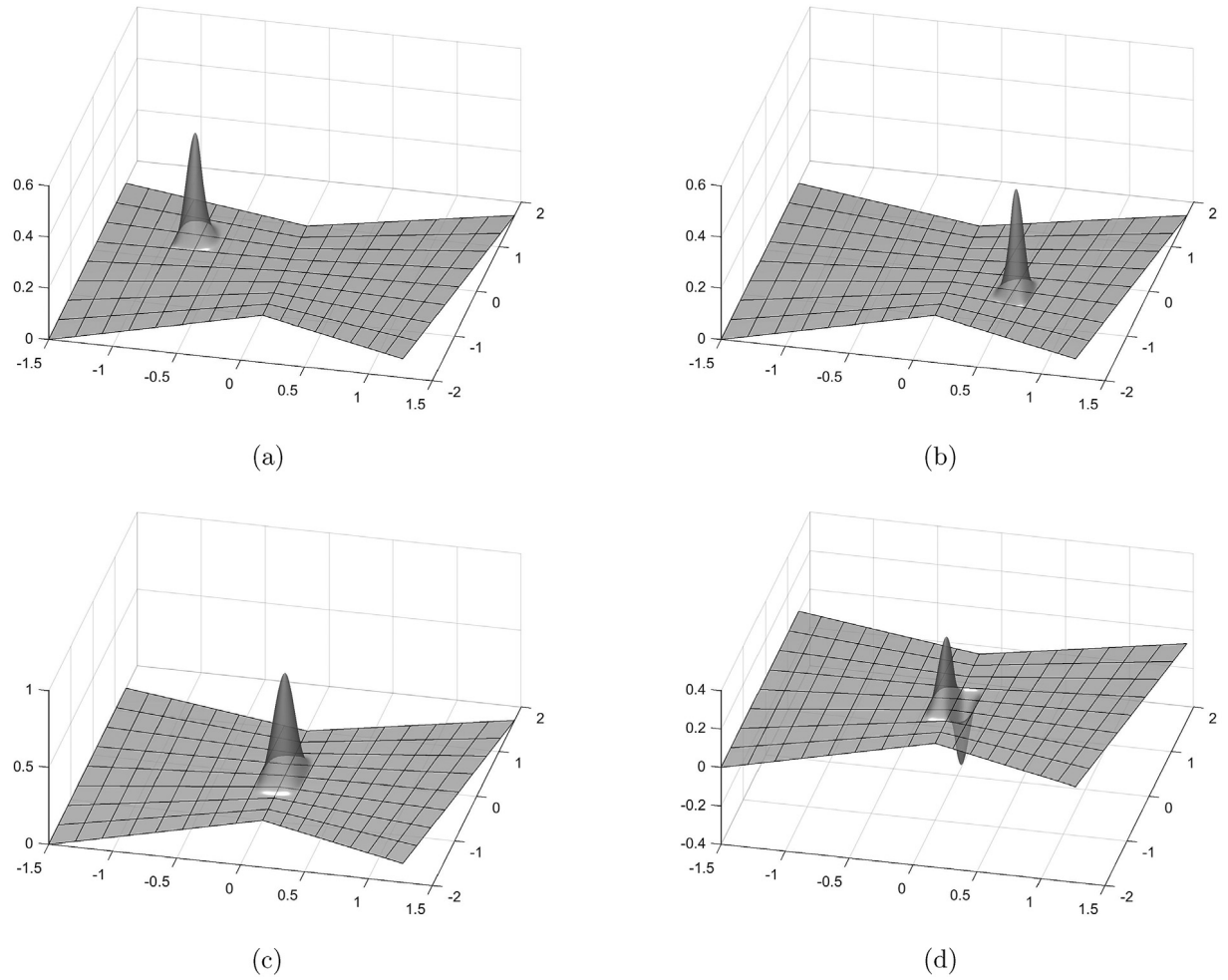

Fig. 1. Example of basis functions of $\mathbb{W}$ on a two-patch domain: figures (a)–(b) show two basis functions of type (13) (standard B-splines whose support is included in one of the two patches), while figures (c) and (d) correspond to basis functions of type (14) and (15), respectively (whose supports intersect the interface).

3.1. Hierarchical splines: abstract definition

Let $\mathbb{U}^0 \subset \mathbb{U}^1 \subset \ldots \subset \mathbb{U}^{N-1}$ be a sequence of N nested multivariate spline spaces defined on a closed domain $D \subset \mathbb{R}^d$, so that any space $\mathbb{U}^\ell$, for $\ell = 0, \ldots, N-1$, is spanned by a (finite) basis Ψ^ℓ satisfying the following properties.

(P1) *Local linear independence*;
(P2) *Local and compact support.*

The first property guarantees that for any subdomain S, the restrictions of the (non-vanishing) functions $\psi \in \Psi^\ell$ to S are linearly independent. The locality of the support instead enables to localize the influence of the basis functions with respect to delimited areas of the domain. Note that the nested nature of the spline spaces implies the existence of a two-scale relation between adjacent bases: for any level ℓ, each basis function in Ψ^ℓ can be expressed as linear combination of basis functions in $\Psi^{\ell+1}$.

By also considering a sequence of closed nested domains

$$\Omega^0 \supseteq \Omega^1 \supseteq \ldots \supseteq \Omega^{N-1}, \tag{17}$$

with $\Omega^0 \subseteq D$, we can define a hierarchical spline basis according to the following definition.

Definition 1. The hierarchical spline basis $\mathcal{H}$ with respect to the domain hierarchy (17) is defined as

$$\mathcal{H} = \left\{ \psi \in \Psi^\ell : \operatorname{supp}^0 \psi \subseteq \Omega^\ell \wedge \operatorname{supp}^0 \psi \not\subseteq \Omega^{\ell+1}, \ell = 0, \ldots, N-1 \right\},$$

where $\operatorname{supp}^0 \psi = \operatorname{supp} \psi \cap \Omega^0$.

Note that the basis $\mathcal{H} = \mathcal{H}^{N-1}$ can be iteratively constructed as follows.

1. $\mathcal{H}^0 = \left\{\psi \in \Psi^0 : \operatorname{supp}^0 \psi \neq \emptyset\right\}$;
2. for $\ell = 0, \dots, N-2$

$$\mathcal{H}^{\ell+1} = \mathcal{H}_A^{\ell+1} \cup \mathcal{H}_B^{\ell+1},$$

where

$$\mathcal{H}_A^{\ell+1} = \left\{\psi \in \mathcal{H}^\ell : \operatorname{supp}^0 \psi \not\subseteq \Omega^{\ell+1}\right\} \quad \text{and} \quad \mathcal{H}_B^{\ell+1} = \left\{\psi \in \Psi^{\ell+1} : \operatorname{supp}^0 \psi \subseteq \Omega^{\ell+1}\right\}.$$

The main properties of the hierarchical basis can be summarized as follows.

Proposition 1. *By assuming that properties (P1)–(P2) hold for the bases Ψ^ℓ, the hierarchical basis satisfies the following properties:*

(i) the functions in $\mathcal{H}$ are linearly independent,
(ii) the intermediate spline spaces are nested, namely $\operatorname{span} \mathcal{H}^\ell \subseteq \operatorname{span} \mathcal{H}^{\ell+1}$,
(iii) given an enlargement of the subdomains $(\widehat{\Omega}^\ell)_{\ell=0,\dots,\widehat{N}-1}$, with $N \leq \widehat{N}$, such that $\Omega^0 = \widehat{\Omega}^0$ and $\Omega^\ell \subseteq \widehat{\Omega}^\ell$, for $\ell = 1, \dots, N-1$, then $\operatorname{span}\mathcal{H} \subseteq \operatorname{span}\widehat{\mathcal{H}}$.

Proof. The proof follows along the same lines as in [15] for hierarchical B-splines. □

Proposition 1 summarizes the key properties of a hierarchical set of basis functions constructed according to Definition 1, when the underlying sequence of bases Ψ^ℓ satisfies only properties (P1)–(P2).

The results in Proposition 1 remain valid when additional assumptions are considered [17]. In particular, if the basis functions in Ψ^ℓ, for $\ell = 0, \dots, N-1$ are *non-negative*, the hierarchical basis functions are also non-negative. Moreover, the partition of unity property in the hierarchical setting can be recovered by considering the *truncated basis* for hierarchical spline spaces [17]. In this case, the partition of unity property at each level ℓ is also required together with the positiveness of the coefficients in the refinement mask. Even if the construction of C^1 functions on two patch geometries considered in the previous section does not satisfy the non-negativity and partition of unity properties, we could still apply the truncation mechanism to reduce the support of coarser basis functions in the C^1 hierarchical basis. Obviously, the resulting truncated basis would not satisfy the other interesting properties of truncated hierarchical B-splines, see [16,17].

3.2. The C^1 hierarchical isogeometric space

By following the construction for the C^1 isogeometric spline space presented in Section 2, we can now introduce its hierarchical extension. We recall that instead of considering the full C^1 space $\mathbb{V}$ at any hierarchical level, we may restrict to the simpler subspace $\mathbb{W}$, whose dimension does not depend on the functions $\alpha^{(L)}$, $\alpha^{(R)}$ and β, and it has analogous approximation properties as the full space.

We consider an initial knot vector $\Xi_p^{r,0} \equiv \Xi_p^r$ as defined in (1) for then introducing the sequence of knot vectors with respect to a fixed degree p

$$\Xi_p^{r,0}, \Xi_p^{r,1} \dots, \Xi_p^{r,N-1},$$

where each knot vector

$$\Xi_p^{r,\ell} = \{ \underbrace{0, \dots, 0}_{(p+1)-\text{times}}, \underbrace{\tau_1^\ell, \dots, \tau_1^\ell}_{(p-r)-\text{times}}, \underbrace{\tau_2^\ell, \dots, \tau_2^\ell}_{(p-r)-\text{times}}, \dots, \underbrace{\tau_{k^\ell}^\ell, \dots, \tau_{k^\ell}^\ell}_{(p-r)-\text{times}}, \underbrace{1, \dots, 1}_{(p+1)-\text{times}} \},$$

for $\ell = 1, \dots, N-1$, is obtained via dyadic refinement of the knot vector of the previous level, keeping the same degree and regularity, and therefore $k^\ell = 2k^{\ell-1} + 1$. We denote by $\mathbb{S}_p^{r,\ell}$ the univariate spline space in $[0, 1]$ with respect to the open knot vector $\Xi_p^{r,\ell}$, and let $N_{i,p}^{r,\ell}$, for $i \in \mathbf{I}^\ell = \{0, \dots, p + k^\ell(p-r)\}$, be the associated B-splines. In addition, as in the one-level case, $\mathbb{S}_p^{r+1,\ell}$ and $\mathbb{S}_{p-1}^{r,\ell}$ ($N_{i,p}^{r+1,\ell}$ and $N_{i,p-1}^{r,\ell}$) indicate the subspaces (and their basis functions) of higher regularity and lower degree, respectively. We also denote by

$$n^\ell = p + 1 + k^\ell(p-r), \quad n_0^\ell = p + 1 + k^\ell(p-r-1), \quad \text{and} \quad n_1^\ell = p + k^\ell(p-r-1),$$

the dimensions of the spline spaces $\mathbb{S}_p^{r,\ell}$, $\mathbb{S}_p^{r+1,\ell}$ and $\mathbb{S}_{p-1}^{r,\ell}$, respectively, and, analogously to $\mathbf{I}^\ell$, we introduce the index sets

$$\mathbf{I}_0^\ell = \{0, \dots, n_0^\ell - 1\}, \qquad \mathbf{I}_1^\ell = \{0, \dots, n_1^\ell - 1\},$$

corresponding to functions in $\mathbb{S}_p^{r+1,\ell}$ and $\mathbb{S}_{p-1}^{r,\ell}$, respectively.

Let

$$\mathbb{V}^0 \subset \mathbb{V}^1 \subset \dots \subset \mathbb{V}^{N-1}$$

be a sequence of nested C^1 isogeometric spline spaces, with $\mathbb{V}^\ell$ defined on the two-patch domain $\Omega = \Omega^{(L)} \cup \Omega^{(R)}$ with respect to the spline space of level ℓ. Analogously to the construction detailed in Section 2.2, for each level $0 \le \ell \le N-1$ let us consider the subspace

$$\mathbb{W}^\ell = \operatorname{span}\Phi^\ell, \quad \text{with } \Phi^\ell = \Phi^\ell_{\Omega^{(L)}} \cup \Phi^\ell_{\Omega^{(R)}} \cup \Phi^\ell_{\Gamma_0} \cup \Phi^\ell_{\Gamma_1},$$

where the basis functions are given by

$$\Phi^\ell_{\Omega^{(S)}} = \left\{ \phi^{\Omega^{(S)}}_{i,j} \ : \ i \in \mathbf{I}^\ell \setminus \{0,1\};\, j \in \mathbf{I}^\ell \right\}, \quad \Phi^\ell_{\Gamma_0} = \left\{ \phi^{\Gamma_0}_i \ : \ i \in \mathbf{I}^\ell_0 \right\}, \quad \Phi^\ell_{\Gamma_1} = \left\{ \phi^{\Gamma_1}_i \ : \ i \in \mathbf{I}^\ell_1 \right\},$$

with $S \in \{L, R\}$, directly defined as in (11) and (12) for the one-level case.

By considering a domain hierarchy as in (17) on the two-patch domain $\Omega \equiv \Omega^0$, and the sets of isogeometric functions Φ^ℓ at different levels, we arrive at the following definition.

Definition 2. The C^1 hierarchical isogeometric space $\mathbb{W}_H$ with respect to a domain hierarchy of the two-patch domain Ω, that satisfies (17) with $\Omega^0 = \Omega$, is defined as

$$\mathbb{W}_H = \operatorname{span} \mathcal{W} \quad \text{with} \quad \mathcal{W} = \left\{ \phi \in \Phi^\ell : \operatorname{supp}^0 \phi \subseteq \Omega^\ell \wedge \operatorname{supp}^0 \phi \not\subseteq \Omega^{\ell+1},\ \ell = 0, \dots, N-1 \right\}.$$

The basis functions are then of the same type as in the tensor-product case, only belonging to different levels, see Fig. 2 for an example.

In the remaining part of this section we want to prove that $\mathcal{W}$ is indeed a basis of the C^1 hierarchical isogeometric space $\mathbb{W}_H$. This requires to verify the properties for the abstract definition given in Section 3.1, in particular the nestedness of the spaces $\mathbb{W}^\ell$, and that the one-level C^1 bases spanning each $\mathbb{W}^\ell$, for $\ell = 0, \dots, N-1$, satisfy the hypotheses of Proposition 1, i.e. properties (P1)–(P2). The nestedness of the spaces $\mathbb{W}^\ell$, $\ell = 0, 1, \dots, N-1$, easily follows from definition (16), as stated in the following Proposition.

Proposition 2. *Let $N \in \mathbb{N}$. The sequence of spaces $\mathbb{W}^\ell$, $\ell = 0, 1, \dots, N-1$, is nested, i.e.*

$$\mathbb{W}^0 \subset \mathbb{W}^1 \subset \dots \subset \mathbb{W}^{N-1}.$$

Proof. Let $\ell = 0, \dots, N-2$, and $\phi \in \mathbb{W}^\ell \subset \mathbb{V}^\ell$. By definition (5) the spaces $\mathbb{V}^\ell$ are nested, hence $\phi \in \mathbb{V}^\ell \subset \mathbb{V}^{\ell+1}$. Since the spline spaces $\mathbb{S}^{r+1,\ell}_p$ and $\mathbb{S}^{r,\ell}_{p-1}$ are nested, too, we have $\phi \circ \mathbf{F}_0 \in \mathbb{S}^{r+1,\ell}_p \subset \mathbb{S}^{r+1,\ell+1}_p$ and $\nabla\phi \cdot (\mathbf{d} \circ \mathbf{F}_0) \in \mathbb{S}^{r,\ell}_{p-1} \subset \mathbb{S}^{r,\ell+1}_{p-1}$, which implies that $\phi \in \mathbb{W}^{\ell+1}$. □

The locality and compactness of the support of these functions in (P2) comes directly by construction and by the same property for standard B-splines, see (13)–(15) and Fig. 1. The property of local linear independence in (P1) instead is proven in the following Proposition.

Proposition 3. *The set of basis functions $\Phi^\ell = \Phi^\ell_{\Omega^{(L)}} \cup \Phi^\ell_{\Omega^{(R)}} \cup \Phi^\ell_{\Gamma_0} \cup \Phi^\ell_{\Gamma_1}$, is locally linearly independent, for $\ell = 0, \dots, N-1$.*

Proof. Since we have to prove the statement for any hierarchical level ℓ, we just remove the superscript ℓ in the proof to simplify the notation. Recall that the functions in Φ are linearly independent. It is well known that the functions in $\Phi_{\Omega^{(L)}} \cup \Phi_{\Omega^{(R)}}$ are locally linearly independent, as they are (mapped) standard B-splines. Furthermore, it is also well known, or easy to verify, that each of the following sets of univariate functions is locally linearly independent

(a) $\{N^r_{0,p} + N^r_{1,p}, N^r_{1,p}\} \cup \{N^r_{i,p}\}_{i \in \mathbf{I} \setminus \{0,1\}}$,
(b) $\{N^{r+1}_{i,p}\}_{i \in \mathbf{I}_0}$,
(c) $\{N^r_{i,p-1}\}_{i \in \mathbf{I}_1}$.

We prove that the set of functions Φ is locally linearly independent, which means that, for any open set $\widetilde{\Omega} \subset \Omega$ the functions of Φ that do not vanish in $\widetilde{\Omega}$ are linearly independent on $\widetilde{\Omega}$. Let $\widetilde{\mathbf{I}}_0 \subset \mathbf{I}_0$, $\widetilde{\mathbf{I}}_1 \subset \mathbf{I}_1$ and $\widetilde{\mathbf{I}}^{(S)}_j \subset \mathbf{I}$, $j \in \mathbf{I} \setminus \{0,1\}$, $S \in \{L, R\}$, be the sets of indices corresponding to those functions $\phi^{\Gamma_0}_i$, $\phi^{\Gamma_1}_i$ and $\phi^{\Omega^{(S)}}_{j,i}$, respectively, that do not vanish on $\widetilde{\Omega}$. Then the equation

$$\sum_{i \in \widetilde{\mathbf{I}}_0} \mu_{0,i} \phi^{\Gamma_0}_i(\mathbf{x}) + \sum_{i \in \widetilde{\mathbf{I}}_1} \mu_{1,i} \phi^{\Gamma_1}_i(\mathbf{x}) + \sum_{S \in \{L,R\}} \sum_{j \in \mathbf{I} \setminus \{0,1\}} \sum_{i \in \widetilde{\mathbf{I}}^{(S)}_j} \mu^{(S)}_{j,i} \phi^{\Omega^{(S)}}_{j,i}(\mathbf{x}) = 0, \quad \mathbf{x} \in \widetilde{\Omega} \tag{18}$$

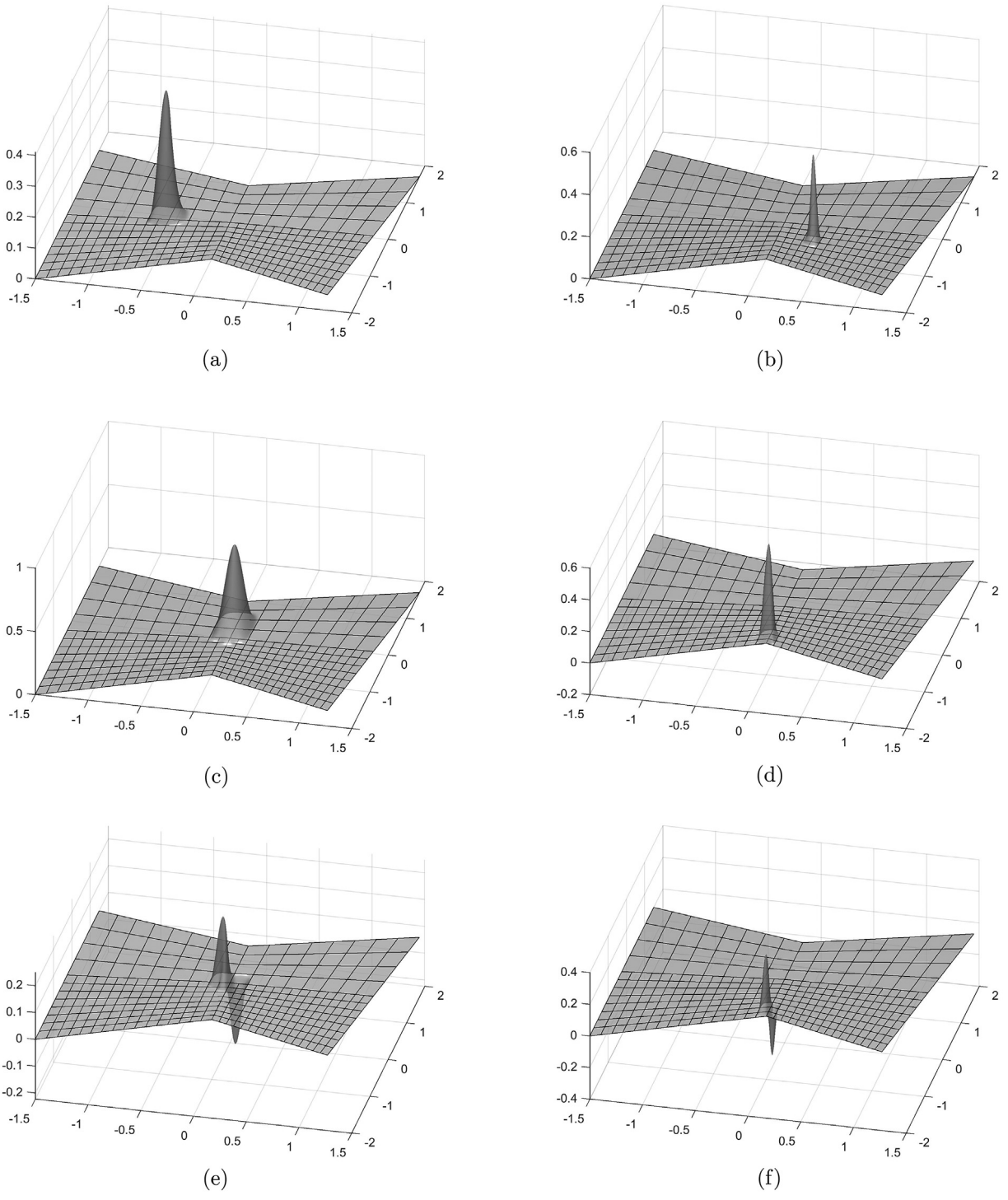

Fig. 2. Example of basis functions of $\mathbb{W}_H$ on a two-patch domain: on the left basis functions of type (13)–(15) respectively belonging to level 0 are shown, while on the right analogous basis functions of level 1 are reported.

has to imply $\mu_{0,i} = 0$ for all $i \in \widetilde{\mathbf{I}}_0$, $\mu_{1,i} = 0$ for all $i \in \widetilde{\mathbf{I}}_1$, and $\mu_{j,i}^{(S)} = 0$ for all $i \in \widetilde{\mathbf{I}}_j^{(S)}$, $j \in \mathbf{I} \setminus \{0, 1\}$, $S \in \{L, R\}$. Eq. (18) implies that

$$\sum_{i\in\widetilde{\mathbf{I}}_0} \mu_{0,i}\Big(\phi_i^{\Gamma_0} \circ \mathbf{F}^{(S)}\Big)(\xi_1, \xi_2) + \sum_{i\in\widetilde{\mathbf{I}}_1} \mu_{1,i}\Big(\phi_i^{\Gamma_1} \circ \mathbf{F}^{(S)}\Big)(\xi_1, \xi_2) + \sum_{j\in\mathbf{I}\setminus\{0,1\}} \sum_{i\in\widetilde{\mathbf{I}}_j^{(S)}} \mu_{j,i}^{(S)}\Big(\phi_{j,i}^{\Omega^{(S)}} \circ \mathbf{F}^{(S)}\Big)(\xi_1, \xi_2) = 0,$$

for $(\xi_1, \xi_2) \in \widetilde{\Omega}^{(S)}$ and $S \in \{L, R\}$, where $\widetilde{\Omega}^{(S)} \subseteq (0, 1)^2$ are the corresponding parameter domains for the geometry mappings $\mathbf{F}^{(S)}$ such that the closure of $\widetilde{\Omega}$ is

$$\mathrm{cl}(\widetilde{\Omega}) = \mathrm{cl}\left(\mathbf{F}^{(L)}(\widetilde{\Omega}^{(L)}) \cup \mathbf{F}^{(R)}(\widetilde{\Omega}^{(R)})\right).$$

By substituting the functions $\phi_i^{\Gamma_0} \circ \mathbf{F}^{(S)}$, $\phi_i^{\Gamma_1} \circ \mathbf{F}^{(S)}$ and $\phi_{j,i}^{\Omega^{(S)}} \circ \mathbf{F}^{(S)}$ by their corresponding expressions, we obtain

$$\begin{aligned}&\sum_{i\in\widetilde{\mathbf{I}}_0} \mu_{0,i}\left(N_{i,p}^{r+1}(\xi_2)\Big(N_{0,p}^{r}(\xi_1) + N_{1,p}^{r}(\xi_1)\Big) + \beta^{(S)}(\xi_2)\Big(N_{i,p}^{r+1}\Big)'(\xi_2)\frac{\tau_1}{p}N_{1,p}^{r}(\xi_1)\right)\\ &+ \sum_{i\in\widetilde{\mathbf{I}}_1} \mu_{1,i}\left(\alpha^{(S)}(\xi_2)N_{i,p-1}^{r}(\xi_2)N_{1,p}^{r}(\xi_1)\right) + \sum_{j\in\mathbf{I}\setminus\{0,1\}} \sum_{i\in\widetilde{\mathbf{I}}_j^{(S)}} \mu_{j,i}^{(S)}N_{j,p}^{r}(\xi_1)N_{i,p}^{r}(\xi_2) = 0,\end{aligned}$$

for $(\xi_1, \xi_2) \in \widetilde{\Omega}^{(S)}$ and $S \in \{L, R\}$, which can be rewritten as

$$\begin{aligned}&\Big(N_{0,p}^{r}(\xi_1) + N_{1,p}^{r}(\xi_1)\Big)\Big(\sum_{i\in\widetilde{\mathbf{I}}_0} \mu_{0,i}N_{i,p}^{r+1}(\xi_2)\Big) + N_{1,p}^{r}(\xi_1)\Big(\frac{\tau_1}{p}\sum_{i\in\widetilde{\mathbf{I}}_0} \mu_{0,i}\beta^{(S)}(\xi_2)\Big(N_{i,p}^{r+1}\Big)'(\xi_2)\Big)\\ &+ N_{1,p}^{r}(\xi_1)\Big(\sum_{i\in\widetilde{\mathbf{I}}_1} \mu_{1,i}\alpha^{(S)}(\xi_2)N_{i,p-1}^{r}(\xi_2)\Big) + \sum_{j\in\mathbf{I}\setminus\{0,1\}} N_{j,p}^{r}(\xi_1)\Big(\sum_{i\in\widetilde{\mathbf{I}}_j^{(S)}} \mu_{j,i}^{(S)}N_{i,p}^{r}(\xi_2)\Big) = 0.\end{aligned} \tag{19}$$

Now, since $\widetilde{\Omega}$ and $\widetilde{\Omega}^{(S)}$ are open, for each $i \in \widetilde{\mathbf{I}}_0$ there exists a point $(\xi_1^{(S)}, \xi_2^{(S)}) \in \widetilde{\Omega}^{(S)}$, with $S \in \{L, R\}$, such that $\phi_i^{\Gamma_0}$ does not vanish in a neighborhood $Q \subset \widetilde{\Omega}^{(S)}$ of the point. Due to the fact that the univariate functions $N_{0,p}^{r} + N_{1,p}^{r}$, $N_{1,p}^{r}$ and $N_{j,p}^{r}$, $j \in \mathbf{I} \setminus \{0, 1\}$ are locally linearly independent and that $N_{0,p}^{r}(\xi_1^{(S)}) + N_{1,p}^{r}(\xi_1^{(S)}) \neq 0$, we get that

$$\sum_{i\in\widetilde{\mathbf{I}}_0} \mu_{0,i}N_{i,p}^{r+1}(\xi_2) = 0, \quad \text{for } \xi_2 \text{ such that } (\xi_1^{(S)}, \xi_2) \in Q.$$

This equation and the local linear independence of the univariate functions $\{N_{i,p}^{r+1}\}_{i\in\widetilde{\mathbf{I}}_0}$ imply that $\mu_{0,i} = 0$. Applying this argument for all $i \in \widetilde{\mathbf{I}}_0$, we obtain $\mu_{0,i} = 0$, $i \in \widetilde{\mathbf{I}}_0$, and the term (19) simplifies to

$$N_{1,p}^{r}(\xi_1)\Big(\sum_{i\in\widetilde{\mathbf{I}}_1} \mu_{1,i}\alpha^{(S)}(\xi_2)N_{i,p-1}^{r}(\xi_2)\Big) + \sum_{j\in\mathbf{I}\setminus\{0,1\}} N_{j,p}^{r}(\xi_1)\Big(\sum_{i\in\widetilde{\mathbf{I}}_j^{(S)}} \mu_{j,i}^{(S)}N_{i,p}^{r}(\xi_2)\Big) = 0. \tag{20}$$

Similarly, we can obtain for each $i \in \widetilde{I}_1$

$$\sum_{i\in\widetilde{\mathbf{I}}_1} \mu_{1,i}\,\alpha^{(S)}(\xi_2)N_{i,p-1}^{r}(\xi_2) = 0, \quad \text{for } \xi_2 \text{ such that } (\xi_1^{(S)}, \xi_2) \in Q, \tag{21}$$

with the corresponding points $(\xi_1^{(S)}, \xi_2) \in \widetilde{\Omega}$ and neighborhoods $Q \subset \widetilde{\Omega}$. Since the function $\alpha^{(S)}$ is just a linear function which never takes the value zero, see (2), Eq. (21) implies that

$$\sum_{i\in\widetilde{\mathbf{I}}_1} \mu_{1,i}\,N_{i,p-1}^{r}(\xi_2) = 0, \quad \text{for } \xi_2 \text{ such that } (\xi_1^{(S)}, \xi_2) \in Q.$$

The local linear independence of the univariate functions $\{N_{i,p-1}^{r}\}_{i\in\widetilde{\mathbf{I}}_1}$ implies as before that $\mu_{1,i} = 0$, $i \in \widetilde{\mathbf{I}}_1$, and therefore the term (20) simplifies further to

$$\sum_{j\in\mathbf{I}\setminus\{0,1\}} N_{j,p}^{r}(\xi_1)\Big(\sum_{i\in\widetilde{\mathbf{I}}_j^{(S)}} \mu_{j,i}^{(S)}N_{i,p}^{r}(\xi_2)\Big) = 0.$$

Finally, $\mu_{j,i}^{(S)} = 0$, $i \in \widetilde{\mathbf{I}}_j^{(S)}$, $j \in \mathbf{I} \setminus \{0, 1\}$, $S \in \{L, R\}$, follows directly from the fact that the functions in $\Phi_{\Omega^{(L)}} \cup \Phi_{\Omega^{(R)}}$ are locally linearly independent. □

Finally, we have all what is necessary to prove the main result.

Theorem 1. *$\mathcal{W}$ is a basis for the C^1 hierarchical space $\mathbb{W}_H$.*

Proof. The result holds because the spaces in Definition 2 satisfy the hypotheses in Proposition 1. In particular, we have the nestedness of the spaces by Proposition 2, and for the basis functions in Φ^ℓ the local linear independence (P1) by Proposition 3, and the local and compact support (P2) by their definition in (13)–(15). □

Remark 2. In contrast to the here considered C^1 basis functions for the case of analysis-suitable G^1 two-patch geometries, the analogous C^1 basis functions for the multi-patch case based on [45] are, in general, not locally linearly dependent. Due to the amount of notation needed and to their technicality, we do not report here counterexamples, but what happens, even in some basic domain configurations, is that the basis functions defined in the vicinity of a vertex may be locally linearly dependent. As a consequence, the construction of a hierarchical C^1 space requires a different approach, whose investigation is beyond the scope of the present paper.

4. Refinement mask and implementation

In this section we give some details about practical aspects regarding the implementation of isogeometric methods based on the hierarchical space $\mathbb{W}_H$. First, we recall how the C^1 basis functions of one level can be expressed as linear combinations of standard B-splines. Then, we specify the refinement masks, which allow to write the basis functions of Φ^ℓ as linear combinations of the basis functions of $\Phi^{\ell+1}$. The refinement masks are important, as they are needed, for instance, for knot insertion algorithms and some operators in multilevel preconditioning. Finally, we focus on the implementation of the hierarchical space in the open Octave/Matlab software GeoPDEs [49], whose principles can be applied almost identically to any other isogeometric code. The implementation employs the refinement masks for the evaluation of basis functions too.

4.1. Representation of the basis with respect to $\mathbb{S}^r_p \otimes \mathbb{S}^r_p$

We describe the strategy shown in [43] to represent the spline functions of Section 2.2, namely $\phi^{\Omega^{(S')}}_{i,j} \circ \mathbf{F}^{(S)}$, $\phi^{\Gamma_0}_i \circ \mathbf{F}^{(S)}$ and $\phi^{\Gamma_1}_i \circ \mathbf{F}^{(S)}$, $S \in \{L, R\}$, with respect to the spline space $\mathbb{S}^r_p \otimes \mathbb{S}^r_p$, using a vectorial notation. Let us first introduce the vectors of functions $\mathbf{N}_0$, $\mathbf{N}_1$ and $\mathbf{N}_2$, given by

$$\mathbf{N}_0(\xi_1,\xi_2) = [N^r_{0,p}(\xi_1)N^r_{j,p}(\xi_2)]_{j\in\mathbf{I}}, \qquad \mathbf{N}_1(\xi_1,\xi_2) = [N^r_{1,p}(\xi_1)N^r_{j,p}(\xi_2)]_{j\in\mathbf{I}},$$

and

$$\mathbf{N}_2(\xi_1,\xi_2) = [N^r_{i,p}(\xi_1)N^r_{j,p}(\xi_2)]^T_{i\in\mathbf{I}\setminus\{0,1\},j\in\mathbf{I}},$$

which represent the whole basis of $\mathbb{S}^r_p \otimes \mathbb{S}^r_p$. Let us also introduce, the vectors of functions

$$\boldsymbol{\phi}_{\Gamma_0}(\mathbf{x}) = [\phi^{\Gamma_0}_i(\mathbf{x})]_{i\in\mathbf{I}_0}, \qquad \boldsymbol{\phi}_{\Gamma_1}(\mathbf{x}) = [\phi^{\Gamma_1}_i(\mathbf{x})]_{i\in\mathbf{I}_1},$$

$$\boldsymbol{\phi}_{\Omega^{(S)}}(\mathbf{x}) = [\phi^{\Omega^{(S)}}_{i,j}(\mathbf{x})]_{i\in\mathbf{I}\setminus\{0,1\};\, j\in\mathbf{I}} \quad \text{for } S \in \{L, R\},$$

and finally, for $S \in \{L, R\}$, the vectors of functions $\widehat{\boldsymbol{\phi}}^{(S)}_{\Gamma_0}$, $\widehat{\boldsymbol{\phi}}^{(S)}_{\Gamma_1}$, $\widehat{\boldsymbol{\phi}}^{(S)}_{\Omega^{(S)}}$, given by

$$\widehat{\boldsymbol{\phi}}^{(S)}_{\Gamma_0}(\xi_1,\xi_2) = [\phi^{\Gamma_0}_i \circ \mathbf{F}^{(S)}(\xi_1,\xi_2)]_{i\in\mathbf{I}_0}, \qquad \widehat{\boldsymbol{\phi}}^{(S)}_{\Gamma_1}(\xi_1,\xi_2) = [\phi^{\Gamma_1}_i \circ \mathbf{F}^{(S)}(\xi_1,\xi_2)]_{i\in\mathbf{I}_1},$$

$$\widehat{\boldsymbol{\phi}}^{(S)}_{\Omega^{(S)}}(\xi_1,\xi_2) = [\phi^{\Omega^{(S)}}_{i,j} \circ \mathbf{F}^{(S)}(\xi_1,\xi_2)]_{i\in\mathbf{I}\setminus\{0,1\};\, j\in\mathbf{I}}.$$

Since the basis functions $\phi^{\Omega^{(S)}}_{i,j}$ are just the "standard" isogeometric functions, the spline functions $\widehat{\boldsymbol{\phi}}^{(S)}_{\Omega^{(S)}}(\xi_1,\xi_2)$ automatically belong to the basis of the spline space $\mathbb{S}^r_p \otimes \mathbb{S}^r_p$, while an analysis of the basis functions in $\widehat{\boldsymbol{\phi}}^{(S)}_{\Gamma_0}(\xi_1,\xi_2)$ and $\widehat{\boldsymbol{\phi}}^{(S)}_{\Gamma_1}(\xi_1,\xi_2)$, leads to the following representation

$$\begin{bmatrix} \widehat{\boldsymbol{\phi}}^{(S)}_{\Gamma_0}(\xi_1,\xi_2) \\ \widehat{\boldsymbol{\phi}}^{(S)}_{\Gamma_1}(\xi_1,\xi_2) \\ \widehat{\boldsymbol{\phi}}^{(S)}_{\Omega^{(S)}}(\xi_1,\xi_2) \end{bmatrix} = \begin{bmatrix} \widehat{B} & \widetilde{B}^{(S)} & 0 \\ 0 & \overline{B}^{(S)} & 0 \\ 0 & 0 & I_{n(n-2)} \end{bmatrix} \begin{bmatrix} \mathbf{N}_0(\xi_1,\xi_2) \\ \mathbf{N}_1(\xi_1,\xi_2) \\ \mathbf{N}_2(\xi_1,\xi_2) \end{bmatrix}, \quad S \in \{L, R\}, \tag{22}$$

where I_m denotes the identity matrix of dimension m, and the other blocks of the matrix take the form $\widehat{B} = [\widehat{b}_{i,j}]_{i\in\mathbf{I}_0,j\in\mathbf{I}}$, $\widetilde{B}^{(S)} = [\widetilde{b}^{(S)}_{i,j}]_{i\in\mathbf{I}_0,j\in\mathbf{I}}$, and $\overline{B}^{(S)} = [\overline{b}^{(S)}_{i,j}]_{i\in\mathbf{I}_1,j\in\mathbf{I}}$. In fact, these are sparse matrices, and by defining the index sets

$$\mathbf{J}_{0,i} = \{j \in \mathbf{I} \ : \ \mathrm{supp}(N^r_{j,p}) \cap \mathrm{supp}(N^{r+1}_{i,p}) \neq \emptyset\}, \quad \text{for } i \in \mathbf{I}_0,$$

and

$$\mathbf{J}_{1,i} = \{j \in \mathbf{I} \ : \ \mathrm{supp}(N^r_{j,p}) \cap \mathrm{supp}(N^r_{i,p-1}) \neq \emptyset\}, \quad \text{for } i \in \mathbf{I}_1,$$

it can be seen that the possible non-zero entries are limited to $\widehat{b}_{i,j}$, $\widetilde{b}^{(S)}_{i,j}$, $i \in \mathbf{I}_0$, $j \in \mathbf{J}_{0,i}$, and $\overline{b}^{(S)}_{i,j}$, $i \in \mathbf{I}_1$, $j \in \mathbf{J}_{1,i}$, respectively.

For the sake of completeness, we explain how to compute these coefficients as suggested in [43]. Let us denote by ζ_m, with $m \in \mathbf{I}$, the Greville abscissae of the univariate spline space $\mathbb{S}^r_p$. Then, for each $S \in \{L, R\}$ and for each $i \in \mathbf{I}_0$ or $i \in \mathbf{I}_1$, the linear factors $\widehat{b}_{i,j}$, $\widetilde{b}^{(S)}_{i,j}$, $j \in \mathbf{J}_{0,i}$, and $\overline{b}^{(S)}_{i,j}$, $j \in \mathbf{J}_{1,i}$, can be obtained by solving the following systems of linear equations

$$\left(\phi_i^{\Gamma_0} \circ \mathbf{F}^{(L)}\right)(0, \zeta_m) = \sum_{j\in\mathbf{J}_{0,i}} \widehat{b}_{i,j} N^r_{j,p}(\zeta_m), \quad m \in \mathbf{J}_{0,i},$$

$$\frac{\tau_1 \partial_1\left(\phi_i^{\Gamma_0} \circ \mathbf{F}^{(S)}\right)(0, \zeta_m)}{p} + \left(\phi_i^{\Gamma_0} \circ \mathbf{F}^{(S)}\right)(0, \zeta_m) = \sum_{j\in\mathbf{J}_{0,i}} \widetilde{b}^{(S)}_{i,j} N^r_{j,p}(\zeta_m), \quad m \in \mathbf{J}_{0,i},$$

and

$$\frac{\tau_1 \partial_1\left(\phi_i^{\Gamma_1} \circ \mathbf{F}^{(L)}\right)(0, \zeta_m)}{p} = \sum_{j\in\mathbf{J}_{1,i}} \overline{b}^{(S)}_{i,j} N^r_{j,p}(\zeta_m), \quad m \in \mathbf{J}_{1,i},$$

respectively, see [43] for more details. Note that the coefficients $\widehat{b}_{i,j}$, $i \in \mathbf{I}_0$, are exactly the spline coefficients of the B-spline $N^{r+1}_{j,p}$ for the spline representation with respect to the space $\mathbb{S}^r_p$, and can also be computed by simple knot insertion.

4.2. Refinement masks

Let us recall the notations and assumptions from Section 3.2 for the multi-level setting of the spline spaces $\mathbb{W}^\ell$, $\ell = 0, 1, \ldots, N-1$, where the upper index ℓ refers to the specific level of refinement. We will use the same upper index in an analogous manner for further notations, which have been mainly introduced in Sections 2.2 and 4.1 for the one-level case, such as for the vectors of functions $\mathbf{N}_0$, $\mathbf{N}_1$, $\mathbf{N}_2$ and $\widehat{\boldsymbol{\phi}}^{(S)}_{\Gamma_0}$, $\widehat{\boldsymbol{\phi}}^{(S)}_{\Gamma_1}$, $\widehat{\boldsymbol{\phi}}^{(S)}_{\Omega^{(S)}}$, $S \in \{L, R\}$, and for the transformation matrices $\widehat{B}$, $\widetilde{B}^{(S)}$ and $\overline{B}^{(S)}$, $S \in \{L, R\}$.

Let $\mathbb{R}_+$ be the set of non-negative real numbers. Based on basic properties of B-splines, there exist refinement matrices (refinement masks) $\Lambda^{r,\ell+1}_p \in \mathbb{R}_+^{n^\ell \times n^{\ell+1}}$, $\Lambda^{r+1,\ell+1}_p \in \mathbb{R}_+^{n^\ell_0 \times n^{\ell+1}_0}$ and $\Lambda^{r,\ell+1}_{p-1} \in \mathbb{R}_+^{n^\ell_1 \times n^{\ell+1}_1}$ such that

$$[N^{r,\ell}_{i,p}(\xi)]_{i\in\mathbf{I}^\ell} = \Lambda^{r,\ell+1}_p [N^{r,\ell+1}_{i,p}(\xi)]_{i\in\mathbf{I}^{\ell+1}},$$

$$[N^{r+1,\ell}_{i,p}(\xi)]_{i\in\mathbf{I}^\ell_0} = \Lambda^{r+1,\ell+1}_p [N^{r+1,\ell+1}_{i,p}(\xi)]_{i\in\mathbf{I}^{\ell+1}_0},$$

and

$$[N^{r,\ell}_{i,p-1}(\xi)]_{i\in\mathbf{I}^\ell_1} = \Lambda^{r,\ell+1}_{p-1} [N^{r,\ell+1}_{i,p-1}(\xi)]_{i\in\mathbf{I}^{\ell+1}_1}.$$

These refinement matrices are banded matrices with a small bandwidth. Furthermore, using an analogous notation to Section 4.1 for the vectors of functions, the refinement mask between the tensor-product spaces $\mathbb{S}^{r,\ell}_p \otimes \mathbb{S}^{r,\ell}_p$ and $\mathbb{S}^{r,\ell+1}_p \otimes \mathbb{S}^{r,\ell+1}_p$ is obtained by refining in each parametric direction as a Kronecker product, and can be written in block-matrix form as

$$\begin{bmatrix} \mathbf{N}^\ell_0(\xi_1,\xi_2) \\ \mathbf{N}^\ell_1(\xi_1,\xi_2) \\ \mathbf{N}^\ell_2(\xi_1,\xi_2) \end{bmatrix} = (\Lambda^{r,\ell+1}_p \otimes \Lambda^{r,\ell+1}_p) \begin{bmatrix} \mathbf{N}^{\ell+1}_0(\xi_1,\xi_2) \\ \mathbf{N}^{\ell+1}_1(\xi_1,\xi_2) \\ \mathbf{N}^{\ell+1}_2(\xi_1,\xi_2) \end{bmatrix} = \begin{bmatrix} \Theta^{\ell+1}_{00} & \Theta^{\ell+1}_{01} & \Theta^{\ell+1}_{02} \\ 0 & \Theta^{\ell+1}_{11} & \Theta^{\ell+1}_{12} \\ 0 & 0 & \Theta^{\ell+1}_{22} \end{bmatrix} \begin{bmatrix} \mathbf{N}^{\ell+1}_0(\xi_1,\xi_2) \\ \mathbf{N}^{\ell+1}_1(\xi_1,\xi_2) \\ \mathbf{N}^{\ell+1}_2(\xi_1,\xi_2) \end{bmatrix}. \tag{23}$$

Note that in case of dyadic refinement (as considered in this work), we have $\Theta^{\ell+1}_{02} = 0$.

The following Proposition provides the relation between basis functions of two consecutive levels, which can be interpreted as follows: while the refinement of standard B-splines of level ℓ of course gives B-splines of level $\ell+1$, by refining basis functions of level ℓ of the other two types we obtain functions of the respective type and standard B-splines of level $\ell+1$.

Proposition 4. *It holds that*

$$\begin{bmatrix} \boldsymbol{\phi}^{\ell}_{\Gamma_0}(\mathbf{x}) \\ \boldsymbol{\phi}^{\ell}_{\Gamma_1}(\mathbf{x}) \\ \boldsymbol{\phi}^{\ell}_{\Omega^{(L)}}(\mathbf{x}) \\ \boldsymbol{\phi}^{\ell}_{\Omega^{(R)}}(\mathbf{x}) \end{bmatrix} = \begin{bmatrix} \Lambda_p^{r+1,\ell+1} & 0 & \widetilde{B}^{(L),\ell}\Theta_{12}^{\ell+1} & \widetilde{B}^{(R),\ell}\Theta_{12}^{\ell+1} \\ 0 & \frac{1}{2}\Lambda_{p-1}^{r,\ell+1} & \overline{B}^{(L),\ell}\Theta_{12}^{\ell+1} & \overline{B}^{(R),\ell}\Theta_{12}^{\ell+1} \\ 0 & 0 & \Theta_{22}^{\ell+1} & 0 \\ 0 & 0 & 0 & \Theta_{22}^{\ell+1} \end{bmatrix} \begin{bmatrix} \boldsymbol{\phi}^{\ell+1}_{\Gamma_0}(\mathbf{x}) \\ \boldsymbol{\phi}^{\ell+1}_{\Gamma_1}(\mathbf{x}) \\ \boldsymbol{\phi}^{\ell+1}_{\Omega^{(L)}}(\mathbf{x}) \\ \boldsymbol{\phi}^{\ell+1}_{\Omega^{(R)}}(\mathbf{x}) \end{bmatrix}. \tag{24}$$

Proof. The idea of the proof is based on first writing the basis functions of level ℓ in terms of standard B-splines of the same level by using (22), and then of level $\ell+1$ by (23). Then, the same functions are written in terms of B-splines of level $\ell+1$, using the expressions given by (13)–(15). Comparing the two expressions, and using again (13)–(15), we finally show that the result is a combination of basis functions of level $\ell+1$.

We first show the refinement relation for the functions $\boldsymbol{\phi}^{\ell}_{\Gamma_0}$. For this, let us consider the corresponding spline functions $\widehat{\boldsymbol{\phi}}^{(S),\ell}_{\Gamma_0}$, $S \in \{L, R\}$. On the one hand, using first relation (22) and then relation (23) with the fact that $\Theta_{02}^{\ell+1} = 0$, we obtain

$$\begin{aligned} \widehat{\boldsymbol{\phi}}^{(S),\ell}_{\Gamma_0}(\xi_1,\xi_2) &= \begin{bmatrix} \widehat{B}^{\ell} & \widetilde{B}^{(S),\ell} & 0 \end{bmatrix} \begin{bmatrix} \mathbf{N}_0^{\ell}(\xi_1,\xi_2) & \mathbf{N}_1^{\ell}(\xi_1,\xi_2) & \mathbf{N}_2^{\ell}(\xi_1,\xi_2) \end{bmatrix}^T \\ &= \begin{bmatrix} \widehat{B}^{\ell} & \widetilde{B}^{(S),\ell} & 0 \end{bmatrix} \begin{bmatrix} \Theta_{00}^{\ell+1} & \Theta_{01}^{\ell+1} & 0 \\ 0 & \Theta_{11}^{\ell+1} & \Theta_{12}^{\ell+1} \\ 0 & 0 & \Theta_{22}^{\ell+1} \end{bmatrix} \begin{bmatrix} \mathbf{N}_0^{\ell+1}(\xi_1,\xi_2) \\ \mathbf{N}_1^{\ell+1}(\xi_1,\xi_2) \\ \mathbf{N}_2^{\ell+1}(\xi_1,\xi_2) \end{bmatrix}, \end{aligned}$$

which is equal to

$$\begin{bmatrix} \widehat{B}^{\ell}\Theta_{00}^{\ell+1} & \widehat{B}^{\ell}\Theta_{01}^{\ell+1} + \widetilde{B}^{(S),\ell}\Theta_{11}^{\ell+1} \end{bmatrix} \begin{bmatrix} \mathbf{N}_0^{\ell+1}(\xi_1,\xi_2) \\ \mathbf{N}_1^{\ell+1}(\xi_1,\xi_2) \end{bmatrix} + \widetilde{B}^{(S),\ell}\Theta_{12}^{\ell+1}\mathbf{N}_2^{\ell+1}(\xi_1,\xi_2). \tag{25}$$

On the other hand, from (14) the functions $\widehat{\boldsymbol{\phi}}^{(S),\ell}_{\Gamma_0}$ possess the form

$$\widehat{\boldsymbol{\phi}}^{(S),\ell}_{\Gamma_0}(\xi_1,\xi_2) = \left[N_{i,p}^{r+1,\ell}(\xi_2)\right]_{i\in\mathbf{I}_0^{\ell}} \left(N_{0,p}^{r,\ell}(\xi_1) + N_{1,p}^{r,\ell}(\xi_1)\right) + \frac{\tau_1^{\ell}}{p}\beta^{(S)}(\xi_2)\left[\left(N_{i,p}^{r+1,\ell}\right)'(\xi_2)\right]_{i\in\mathbf{I}_0^{\ell}} N_{1,p}^{r,\ell}(\xi_1).$$

By refining the B-spline functions $N_{i,p}^{r+1,\ell+1}(\xi_2)$, we obtain

$$\begin{aligned} \widehat{\boldsymbol{\phi}}^{(S),\ell}_{\Gamma_0}(\xi_1,\xi_2) = {} & \Lambda_p^{r+1,\ell+1}\left[N_{i,p}^{r+1,\ell+1}(\xi_2)\right]_{i\in\mathbf{I}_0^{\ell+1}} \left(N_{0,p}^{r,\ell}(\xi_1) + N_{1,p}^{r,\ell}(\xi_1)\right) \\ & + \frac{\tau_1^{\ell}}{p}\beta^{(S)}(\xi_2)\Lambda_p^{r+1,\ell+1}\left[\left(N_{i,p}^{r+1,\ell+1}\right)'(\xi_2)\right]_{i\in\mathbf{I}_0^{\ell+1}} N_{1,p}^{r,\ell}(\xi_1). \end{aligned}$$

Then, refining the B-spline functions $N_{0,p}^{r,\ell}(\xi_1) + N_{1,p}^{r,\ell}(\xi_1)$ and $N_{1,p}^{r,\ell}(\xi_1)$ leads to

$$\begin{aligned} \widehat{\boldsymbol{\phi}}^{(S),\ell}_{\Gamma_0}(\xi_1,\xi_2) = {} & \Lambda_p^{r+1,\ell+1}\left[N_{i,p}^{r+1,\ell+1}(\xi_2)\right]_{i\in\mathbf{I}_0^{\ell+1}} \left(\sum_{j\in\mathbf{I}^{\ell+1}} \lambda_{0,j}^{\ell+1} N_{j,p}^{r,\ell+1}(\xi_1) + \sum_{j\in\mathbf{I}^{\ell+1}} \lambda_{1,j}^{\ell+1} N_{j,p}^{r,\ell+1}(\xi_1)\right) \\ & + \frac{\tau_1^{\ell}}{p}\beta^{(S)}(\xi_2)\Lambda_p^{r+1,\ell+1}\left[\left(N_{i,p}^{r+1,\ell+1}\right)'(\xi_2)\right]_{i\in\mathbf{I}_0^{\ell+1}} \sum_{j\in\mathbf{I}^{\ell+1}} \lambda_{1,j}^{\ell+1} N_{j,p}^{r,\ell+1}(\xi_1), \end{aligned}$$

where $\lambda_{i,j}^{\ell+1}$ are the entries of the refinement matrix $\Lambda_p^{r,\ell+1}$. Since we refine dyadically, we have $\lambda_{0,0}^{\ell+1} = 1$, $\lambda_{0,1}^{\ell+1} = \frac{1}{2}$, $\lambda_{1,0}^{\ell+1} = 0$, $\lambda_{1,1}^{\ell+1} = \frac{1}{2}$ and $\tau_1^{\ell+1} = \frac{\tau_1^{\ell}}{2}$, and we get

$$\begin{aligned} \widehat{\boldsymbol{\phi}}^{(S),\ell}_{\Gamma_0}(\xi_1,\xi_2) = {} & \left(\Lambda_p^{r+1,\ell+1}\left[N_{i,p}^{r+1,\ell+1}(\xi_2)\right]_{i\in\mathbf{I}_0^{\ell+1}} \left(N_{0,p}^{r,\ell+1}(\xi_1) + N_{1,p}^{r,\ell+1}(\xi_1)\right)\right. \\ & \left. + \frac{\tau_1^{\ell+1}}{p}\beta^{(S)}(\xi_2)\Lambda_p^{r+1,\ell+1}\left[\left(N_{i,p}^{r+1,\ell+1}\right)'(\xi_2)\right]_{i\in\mathbf{I}_0^{\ell+1}} N_{1,p}^{r,\ell+1}(\xi_1)\right) \\ & + \left(\Lambda_p^{r+1,\ell+1}\left[N_{i,p}^{r+1,\ell+1}(\xi_2)\right]_{i\in\mathbf{I}_0^{\ell+1}} \left(\sum_{j\in\mathbf{I}^{\ell+1}\setminus\{0,1\}} (\lambda_{0,j}^{\ell+1} + \lambda_{1,j}^{\ell+1}) N_{j,p}^{r,\ell+1}(\xi_1)\right)\right. \\ & \left. + \frac{\tau_1^{\ell}}{p}\beta^{(S)}(\xi_2)\Lambda_p^{r+1,\ell+1}\left[\left(N_{i,p}^{r+1,\ell+1}\right)'(\xi_2)\right]_{i\in\mathbf{I}_0^{\ell+1}} \sum_{j\in\mathbf{I}^{\ell+1}\setminus\{0,1\}} \lambda_{1,j}^{\ell+1} N_{j,p}^{r,\ell+1}(\xi_1)\right), \end{aligned}$$

which is equal to

$$\begin{aligned}\widehat{\boldsymbol{\phi}}^{(S),\ell}_{\Gamma_0}(\xi_1,\xi_2) &= \Lambda_p^{r+1,\ell+1}\widehat{\boldsymbol{\phi}}^{(S),\ell+1}_{\Gamma_0}(\xi_1,\xi_2)\\ &+\left(\Lambda_p^{r+1,\ell+1}\left[N_{i,p}^{r+1,\ell+1}(\xi_2)\right]_{i\in\mathbf{I}_0^{\ell+1}}\left(\sum_{j\in\mathbf{I}^{\ell+1}\setminus\{0,1\}}(\lambda_{0,j}^{\ell+1}+\lambda_{1,j}^{\ell+1})N_{j,p}^{r,\ell+1}(\xi_1)\right)\right.\\ &\left.+\frac{\tau_1^\ell}{p}\beta^{(S)}(\xi_2)\Lambda_p^{r+1,\ell+1}\left[\left(N_{i,p}^{r+1,\ell+1}\right)'(\xi_2)\right]_{i\in\mathbf{I}_0^{\ell+1}}\sum_{j\in\mathbf{I}^{\ell+1}\setminus\{0,1\}}\lambda_{1,j}^{\ell+1}N_{j,p}^{r,\ell+1}(\xi_1)\right).\end{aligned}\tag{26}$$

By analyzing the two equal value terms (25) and (26) with respect to the spline representation in ξ_1-direction formed by the B-splines $N_{j,p}^{r,\ell+1}(\xi_1)$, $j\in\mathbf{I}$, one can observe that the first terms in both equations only contain these B-splines with index $j=0,1$, while the second terms only contain these B-splines with indices $j\neq 0,1$. Therefore, both first terms and both second terms each must coincide. This leads to

$$\widehat{\boldsymbol{\phi}}^{(S),\ell}_{\Gamma_0}(\xi_1,\xi_2) = \Lambda_p^{r+1,\ell+1}\widehat{\boldsymbol{\phi}}^{(S),\ell+1}_{\Gamma_0}(\xi_1,\xi_2)+\widetilde{B}^{(S),\ell}\Theta_{12}^{\ell+1}\mathbf{N}_2^{\ell+1}(\xi_1,\xi_2),$$

which directly implies the refinement relation for the functions $\boldsymbol{\phi}^\ell_{\Gamma_0}$.

The refinement for the functions $\boldsymbol{\phi}^\ell_{\Gamma_1}$ can be proven similarly. Considering the spline functions $\widehat{\boldsymbol{\phi}}^{(S),\ell}_{\Gamma_1}$, $S\in\{L,R\}$, we get, on the one hand, by using relations (22) and (23) and the fact that $\Theta_{02}^{\ell+1}=0$

$$\begin{aligned}\widehat{\boldsymbol{\phi}}^{(S),\ell}_{\Gamma_1}(\xi_1,\xi_2) &= \begin{bmatrix}0 & \overline{B}^{(S),\ell} & 0\end{bmatrix}\begin{bmatrix}\mathbf{N}_0^\ell(\xi_1,\xi_2) & \mathbf{N}_1^\ell(\xi_1,\xi_2) & \mathbf{N}_2^\ell(\xi_1,\xi_2)\end{bmatrix}^T\\ &= \begin{bmatrix}0 & \overline{B}^{(S),\ell} & 0\end{bmatrix}\begin{bmatrix}\Theta_{00}^{\ell+1} & \Theta_{01}^{\ell+1} & 0\\ 0 & \Theta_{11}^{\ell+1} & \Theta_{12}^{\ell+1}\\ 0 & 0 & \Theta_{22}^{\ell+1}\end{bmatrix}\begin{bmatrix}\mathbf{N}_0^{\ell+1}(\xi_1,\xi_2)\\ \mathbf{N}_1^{\ell+1}(\xi_1,\xi_2)\\ \mathbf{N}_2^{\ell+1}(\xi_1,\xi_2)\end{bmatrix}\\ &= \overline{B}^{(S),\ell}\Theta_{11}^{\ell+1}\mathbf{N}_1^{\ell+1}(\xi_1,\xi_2)+\overline{B}^{(S),\ell}\Theta_{12}^{\ell+1}\mathbf{N}_2^{\ell+1}(\xi_1,\xi_2).\end{aligned}\tag{27}$$

On the other hand, from (15) the functions $\widehat{\boldsymbol{\phi}}^{(S),\ell}_{\Gamma_1}$ can be expressed as

$$\widehat{\boldsymbol{\phi}}^{(S),\ell}_{\Gamma_1}(\xi_1,\xi_2) = \alpha^{(S)}(\xi_2)\left[N_{i,p-1}^{r,\ell}(\xi_2)\right]_{i\in\mathbf{I}_1^\ell}N_{1,p}^{r,\ell}(\xi_1),$$

and after refining the B-spline functions $N_{1,p}^{r,\ell}(\xi_1)$ and $N_{i,p-1}^{r,\ell}(\xi_2)$, $i\in\mathbf{I}_1^\ell$ we obtain that this is equal to

$$\widehat{\boldsymbol{\phi}}^{(S),\ell}_{\Gamma_1}(\xi_1,\xi_2) = \alpha^{(S)}(\xi_2)\,\Lambda_{p-1}^{r,\ell+1}\left[N_{i,p-1}^{r,\ell+1}(\xi_2)\right]_{i\in\mathbf{I}_1^{\ell+1}}\sum_{j\in\mathbf{I}^{\ell+1}}\lambda_{1,j}^{\ell+1}N_{j,p}^{r,\ell+1}(\xi_1),$$

where $\lambda_{i,j}^{\ell+1}$ are again the entries of the refinement matrix $\Lambda_p^{r,\ell+1}$. Recalling that $\lambda_{1,0}^{\ell+1}=0$ and $\lambda_{1,1}^{\ell+1}=\frac{1}{2}$, we get

$$\begin{aligned}\widehat{\boldsymbol{\phi}}^{(S),\ell}_{\Gamma_1}(\xi_1,\xi_2) &= \alpha^{(S)}(\xi_2)\,\Lambda_{p-1}^{r,\ell+1}\left[N_{i,p-1}^{r,\ell+1}(\xi_2)\right]_{i\in\mathbf{I}_1^{\ell+1}}\left(\frac{1}{2}N_{1,p}^{r,\ell+1}(\xi_1)+\sum_{j\in\mathbf{I}^{\ell+1}\setminus\{0,1\}}\lambda_{1,j}^{\ell+1}N_{j,p}^{r,\ell+1}(\xi_1)\right)\\ &= \frac{1}{2}\Lambda_{p-1}^{r,\ell+1}\widehat{\boldsymbol{\phi}}^{(S),\ell+1}_{\Gamma_1}(\xi_1,\xi_2)+\alpha^{(S)}(\xi_2)\,\Lambda_{p-1}^{r,\ell+1}\left[N_{i,p-1}^{r,\ell+1}(\xi_2)\right]_{i\in\mathbf{I}_1^{\ell+1}}\sum_{j\in\mathbf{I}^{\ell+1}\setminus\{0,1\}}\lambda_{1,j}^{\ell+1}N_{j,p}^{r,\ell+1}(\xi_1).\end{aligned}\tag{28}$$

Considering the two equal value terms (27) and (28), one can argue as for the case of the functions $\widehat{\boldsymbol{\phi}}^{(S),\ell}_{\Gamma_0}$, that both first terms and both second terms each must coincide. This implies

$$\widehat{\boldsymbol{\phi}}^{(S),\ell}_{\Gamma_1}(\xi_1,\xi_2) = \frac{1}{2}\Lambda_{p-1}^{r,\ell+1}\widehat{\boldsymbol{\phi}}^{(S),\ell+1}_{\Gamma_1}(\xi_1,\xi_2)+\overline{B}^{(S),\ell}\Theta_{12}^{\ell+1}\mathbf{N}_2^{\ell+1}(\xi_1,\xi_2),$$

which finally shows the refinement relation for the functions $\boldsymbol{\phi}^\ell_{\Gamma_1}$.

Finally, the relation for the functions $\boldsymbol{\phi}^\ell_{\Omega^{(S)}}$, $S\in\{L,R\}$, directly follows from relation (23), since they correspond to "standard" B-splines. □

4.3. Details about the implementation

The implementation of GeoPDEs is based on two main structures: the mesh, that contains the information related to the computational geometry and the quadrature, and that did not need any change; and the space, with the necessary information to evaluate the basis functions and their derivatives. The new implementation was done in two steps: we first introduced the space of C^1 basis functions of one single level, as in Section 2.2, and then we added the hierarchical construction.

For the space of one level, we created a new space structure that contains the numbering for the basis functions of the three different types, namely $\Phi_{\Omega^{(S)}}$, Φ_{Γ_0} and Φ_{Γ_1}. Note that the number of basis functions of each type is easily obtained from (11)–(12) and the cardinality of the sets of indices $\mathbf{I}$, $\mathbf{I}_0$ and $\mathbf{I}_1$. The evaluation of the basis functions, and also matrix assembly, is performed using the representation of C^1 basis functions in terms of standard tensor-product B-splines, as in Section 4.1. Indeed, one can first assemble the matrix for tensor-product B-splines, and then multiply on each side this matrix by the same matrix given in (22), in the form

$$K_{\mathbb{W}}^{(S)} = B^{(S)} K_{\mathbb{S}}^{(S)} (B^{(S)})^{\top}, \quad \text{with } B^{(S)} = \begin{bmatrix} \widehat{B} & \widetilde{B}^{(S)} & 0 \\ 0 & \overline{B}^{(S)} & 0 \\ 0 & 0 & I_{n(n-2)} \end{bmatrix}, \text{ for } S = L, R,$$

where $K_{\mathbb{S}}^{(S)}$ represents the stiffness matrix for the standard tensor-product B-spline space on the patch $\Omega^{(S)}$, and $K_{\mathbb{W}}^{(S)}$ is the contribution to the stiffness matrix for the $\mathbb{W}$ space from the same patch. Obviously, the same can be done at the element level, by restricting the matrices to suitable submatrices using the indices of non-vanishing functions on the element.

Once the C^1 space of one level is in place, the next step is the implementation of the hierarchical C^1 space, which can be done following [22]. As explained in that paper, although the details were given for standard hierarchical B-splines, the same data structures and algorithms are valid for the abstract construction of hierarchical splines from [17], that we summarized in Section 3.1. As before, the structure for the hierarchical mesh does not differ from the case of hierarchical B-splines, and the differences are in the space structure.

For the space, it is first necessary to complete the space structure of one single level, that we have just described, with some functionality to compute the support of a given basis function, as explained in [22, Section 5.1]. This can be easily done from the analogous functions for B-splines combined with the knowledge of the matrix $B^{(S)}$. Second, the hierarchical structures are constructed following the description in the same paper, except that for the evaluation of basis functions, and in particular for matrix assembly, we make use of the refinement masks of Section 4.2. The support functionality contains all the necessary information to compute the set of active functions when applying the refinement algorithms in [22], while the refinement masks also give us the two-level relation, stored in the matrix $C_\ell^{\ell+1}$ of that paper, that is used both during matrix assembly and to compute the refinement matrix after enlargement of the subdomains.

5. Numerical examples

We present now some numerical examples to show the good performance of the hierarchical C^1 spaces for their use in combination with adaptive methods. We consider two different kinds of numerical examples: the first three tests are run for Poisson problems with an automatic adaptive scheme, while in the last numerical test we solve the bilaplacian problem, with a pre-defined refinement scheme.

5.1. Poisson Problem

The first three examples are tests on the Poisson equation

$$\begin{cases} -\Delta u = f & \text{in } \Omega, \\ u = g & \text{on } \partial\Omega. \end{cases}$$

The goal is to show that using the C^1 space basis does not spoil the properties of the local refinement, and that the behavior is similar to the one obtained using spaces with C^0 continuity across the interfaces. The employed isogeometric algorithm is based on the adaptive loop (see, e.g., [50])

SOLVE $\longrightarrow$ ESTIMATE $\longrightarrow$ MARK $\longrightarrow$ REFINE.

In particular, for the examples we *solve* the variational formulation of the problem imposing the Dirichlet boundary condition by Nitsche's method, and the problem is to find $u_h \in \mathbb{W}_H$ such that for every test function $v_h \in \mathbb{W}_H$ it holds

$$\int_\Omega \nabla u_h \cdot \nabla v_h - \int_{\Gamma_D} \frac{\partial u_h}{\partial \mathbf{n}} v_h - \int_{\Gamma_D} u_h \frac{\partial v_h}{\partial \mathbf{n}} + \int_{\Gamma_D} \frac{\gamma}{h_Q} u_h v_h = \int_\Omega f v_h - \int_{\Gamma_D} g \frac{\partial v_h}{\partial \mathbf{n}} + \int_{\Gamma_D} \frac{\gamma}{h_Q} g v_h,$$

where h_Q is the local element size, and the penalization parameter is chosen as $\gamma = 10(p+1)$, with p the degree. The *error estimate* is computed with a residual-based estimator, given by

$$\varepsilon(u_h) = \left(\sum_{Q \in \mathcal{M}} \varepsilon_Q^2(u_h) \right)^{1/2}, \text{ with } \varepsilon_Q^2(u_h) = \left(h_Q^2 \int_Q |f + \Delta u_h|^2 + h_Q \int_{\partial Q \cap \Gamma} \left[\!\left[\frac{\partial u_h}{\partial \mathbf{n}_\Gamma} \right]\!\right]^2 \right)^{1/2},$$

where the sum is over all the elements of the mesh $\mathcal{M}$, $\mathbf{n}_\Gamma$ is the unit normal vector of the interface Γ, and $[\![\cdot]\!]$ denotes the jump across the interface. Note that for C^1 functions the jump term does not need to be computed. The *marking* of the elements at each iteration is done using Dörfler's strategy (when not stated otherwise, we set the marking parameter equal to 0.75). The *refinement* step of the loop dyadically refines all the marked elements. Although optimal convergence

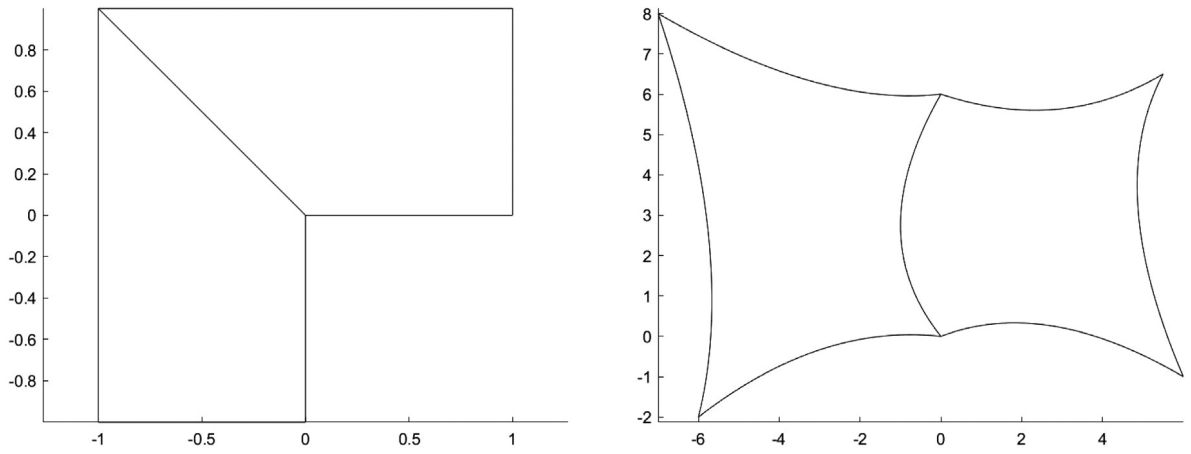

(a) Domain used in the Examples 1 and 4. (b) Domain used in the Examples 2 and 3.

Fig. 3. The two domains used in the numerical examples.

can be only proved if we refine using a refinement strategy that guarantees that meshes are admissible [18], previous numerical results show also a good behavior of non-admissible meshes [50].

For each of the three examples we report the results for degrees $\mathbf{p} = (3, 3), (4, 4)$, with C^1 smoothness across the interface, and with a regularity r equal to degree minus two within the single patches. We compare the results for the adaptive scheme with those obtained by refining uniformly, to show the benefits of local refinement. We also compare them with the ones obtained by employing the same adaptive scheme for hierarchical spaces with C^0 continuity across the interface, while the same regularity within the patches as above is kept, to validate the optimal convergence of the adaptive scheme with C^1 continuity spaces.

Example 1. For the first numerical example we consider the classical L-shaped domain $[-1, 1]^2 \setminus (0, 1) \times (-1, 0)$ defined by two patches as depicted in Fig. 3(a), and the right-hand side f and the boundary condition g are chosen such that the exact solution is given by

$$u(\rho, \theta) = \rho^{\frac{4}{3}} \sin\left(\frac{4}{3}\theta\right),$$

with ρ and θ the polar coordinates. As it is well known, the exact solution has a singularity at the reentrant corner.

We start the adaptive simulation with a coarse mesh of 4×4 elements on each patch, and we use Dörfler's parameter equal to 0.90 for the marking of the elements. The convergence results are presented in Fig. 4. It can be seen that the error in H^1 semi-norm and the estimator converge with the expected rate, in terms of the degrees of freedom, both for the C^1 and the C^0 discretization, and that this convergence rate is better than the one obtained with uniform refinement. The effectivity index of the residual estimator, that is, the ratio between the estimated error and the exact error is around 10, as already observed in previous works [20,50]. Moreover, the errors for the C^1 and the C^0 discretizations are very similar, although slightly better for the C^1 case, which maintains the optimal convergence rate. Note that, since the spaces only differ near the interface, the difference in the error between the two discretizations is very small.

We also show in Fig. 5 the final meshes obtained with the different discretizations. It is clear that the adaptive method correctly refines the mesh in the vicinity of the reentrant corner, where the singularity occurs, and the refinement gets more local with higher degree.

Example 2. In the second example the data of the problem are chosen in such a way that the exact solution is

$$u(x, y) = (-120x + x^2 - 96y - 8xy + 16y^2)^{12/5} \cos(\pi y/20),$$

defined on the domain shown in Fig. 3(b). The geometry of the domain is given by two bicubic Bézier patches, and the control points are chosen following the algorithm in [39], in such a way that the geometry is given by an analysis-suitable G^1 parameterization, see Appendix for details. Note that we have chosen the solution such that it has a singularity along the interface. In this example we start the adaptive simulation with a coarse mesh of 8×8 elements on each patch. We present the convergence results in Fig. 6. As before, both the (relative) error and the estimator converge with optimal rate, and both for the C^0 and the C^1 discretizations, with slightly better result for the C^1 spaces. We note that, since the singularity occurs along a line, optimal order of convergence for higher degrees cannot be obtained without anisotropic refinement, as it was observed in the numerical examples in [51, Section 4.6].

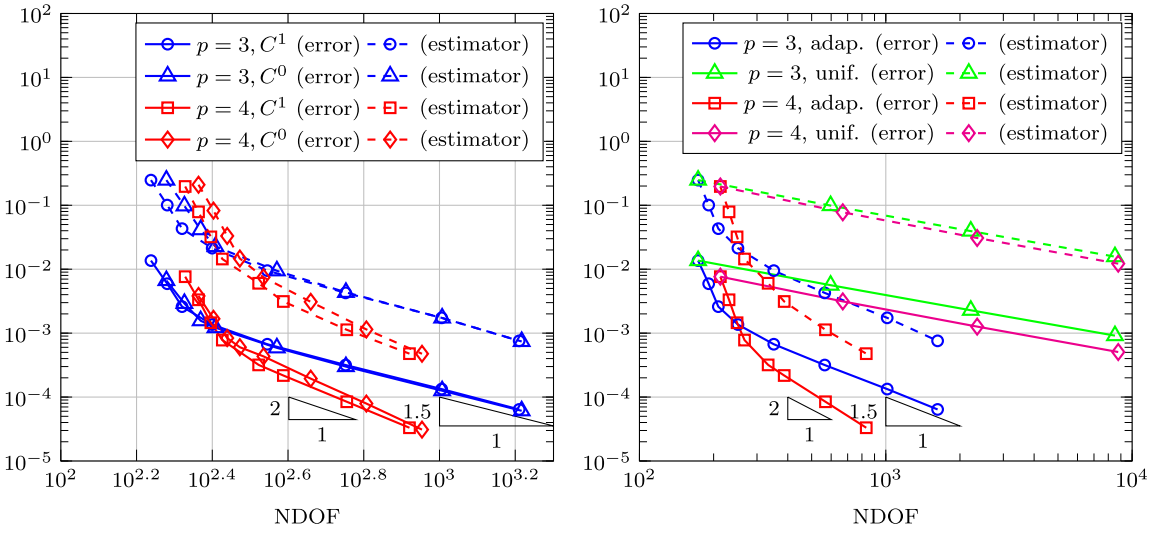

Fig. 4. Error in H^1 semi-norm and estimator for Example 1 with $\mathbf{p} = (3, 3)$ and $\mathbf{p} = (4, 4)$, compared with C^0 case (left) and with global refinement case (right).

We also present in Fig. 7 the finest meshes obtained with the different discretizations, and it can be observed that the adaptive method correctly refines near the interface, where the singularity occurs.

Example 3. We consider the same domain as in the previous example, and the right-hand side and the boundary condition are chosen in such a way that the exact solution is given by

$$u(x, y) = (y - 1.7)^{12/5} \cos(x/4).$$

In this case the solution has a singularity along the line $y = 1.7$, that crosses the interface and is not aligned with the mesh.

The convergence results, that are presented in Fig. 8, are very similar to the ones of the previous example, and show optimal convergence rates for both the C^1 and the C^0 discretizations. As before, we also present in Fig. 9 the finest meshes obtained with the different discretizations. It is evident that the adaptive algorithm successfully refines along the singularity line.

Condition number. To show that C^1 continuity does not reduce the performance of the method compared to C^0 continuity, we have also analyzed the condition number of the corresponding stiffness matrices. In Fig. 10 we show the condition number of the stiffness matrix for the numerical tests of Example 1 and Example 2. The reported results correspond, both for the C^0 and the C^1 case, to the solutions obtained by applying the inexpensive diagonal scaling as preconditioner. The results show a good behavior of the C^1 spaces, with a condition number very similar to the C^0 ones. Note that, due the local nature of the refinement, in many cases the condition number may remain low even without using a more suitable preconditioner.

5.2. Bilaplacian problem

In the last example we consider the solution of the bilaplacian problem, given in strong form by

$$\begin{cases} \Delta^2 u = f & \text{in } \Omega, \\ u = g_1 & \text{on } \partial\Omega, \\ \dfrac{\partial u}{\partial n} = g_2 & \text{on } \partial\Omega. \end{cases}$$

It is well known that the weak formulation of the problem in direct form requires the trial and test functions to be in $H^2(\Omega)$. For the discretization with a Galerkin method, this can be obtained if the discrete basis functions are C^1, and this is the main advantage of the construction of the C^1 hierarchical basis. The solution of the problem with C^0 basis functions, instead, requires to use a mixed variational formulation or some sort of weak enforcement of the C^1 continuity across the interface, like with a Nitsche's method.

Example 4. For the last numerical test we solve the bilaplacian problem in the L-shaped domain as depicted in Fig. 3(a). The right-hand side and the boundary conditions are chosen in such a way that the exact solution is given, in polar

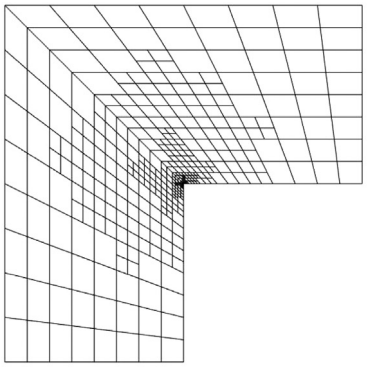

(a) $\mathbf{p} = (3,3)$, C^0 functions on the interface: NDOF=1648.

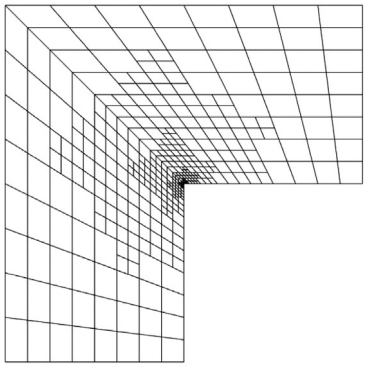

(b) $\mathbf{p} = (3,3)$, C^1 functions on the interface: NDOF=1623.

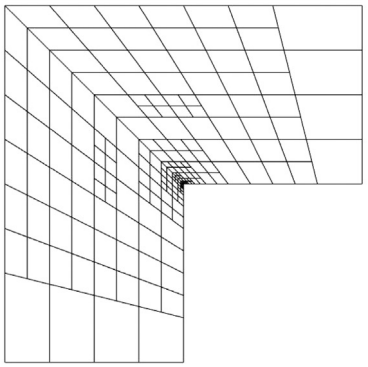

(c) $\mathbf{p} = (4,4)$, C^0 functions on the interface: NDOF=833.

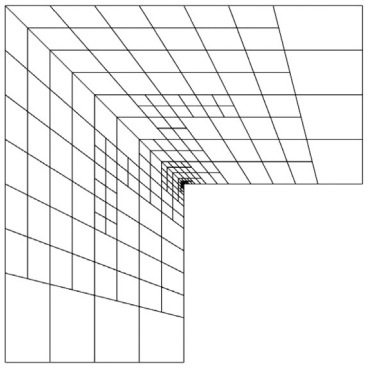

(d) $\mathbf{p} = (4,4)$, C^1 functions on the interface: NDOF=833.

Fig. 5. Hierarchical meshes for Example 1, with $\mathbf{p} = (3,3)$ and $\mathbf{p} = (4,4)$. Apparently the meshes are the same for the C^0 and C^1 case, but there are some differences in the finest levels.

coordinates (ρ, θ), by

$$u(\rho,\theta) = \rho^{z+1}(C_1 F_1(\theta) - C_2 F_2(\theta)),$$

where value in the exponent is chosen equal to $z = 0.544483736782464$, which is the smallest positive solution of

$$\sin(z\omega) + z\sin(\omega) = 0,$$

with $\omega = 3\pi/2$ for the L-shaped domain, see [52, Section 3.4]. The other terms are given by

$$C_1 = \frac{1}{z-1}\sin\left(\frac{3(z-1)\pi}{2}\right) - \frac{1}{z-1}\sin\left(\frac{3(z+1)\pi}{2}\right),$$

$$C_2 = \cos\left(\frac{3(z-1)\pi}{2}\right) - \cos\left(\frac{3(z+1)\pi}{2}\right),$$

$$F_1(\theta) = \cos((z-1)\theta) - \cos((z+1)\theta),$$

$$F_2(\theta) = \frac{1}{z-1}\sin((z-1)\theta) - \frac{1}{z+1}\sin((z+1)\theta).$$

The exact solution has a singularity at the reentrant corner, and it is the same kind of singularity that one would encounter for the Stokes problem.

For our numerical test we start with a coarse mesh of 8×8 elements on each patch. In this case, instead of refining the mesh with an adaptive algorithm we decided to refine following a pre-defined strategy: at each refinement step, a

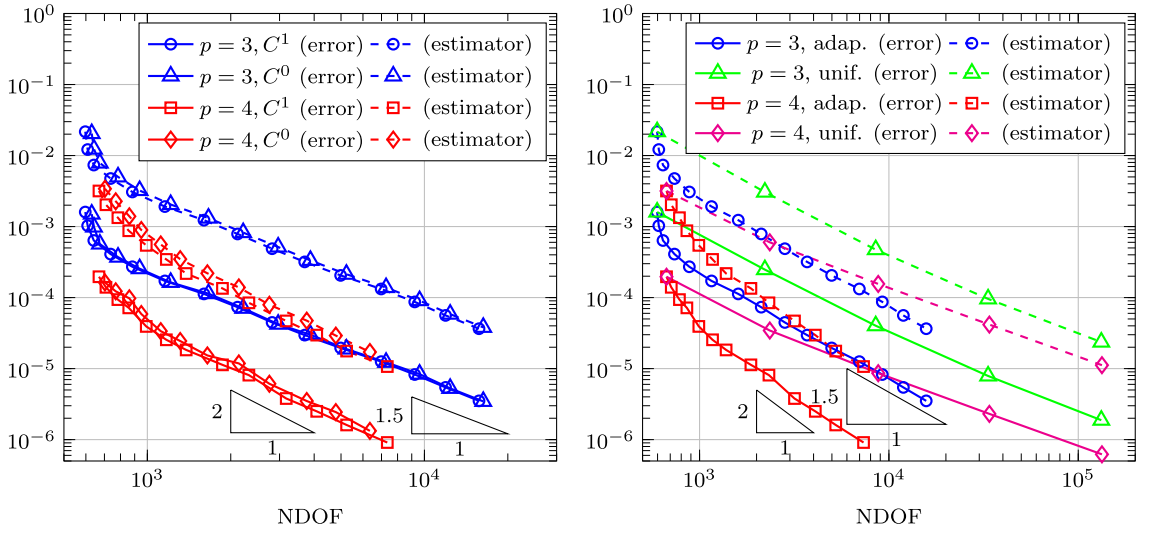

Fig. 6. Relative error in H^1 semi-norm and corresponding estimator for Example 2 with $\mathbf{p} = (3, 3)$ and $\mathbf{p} = (4, 4)$, compared with C^0 case (left) and with global refinement case (right).

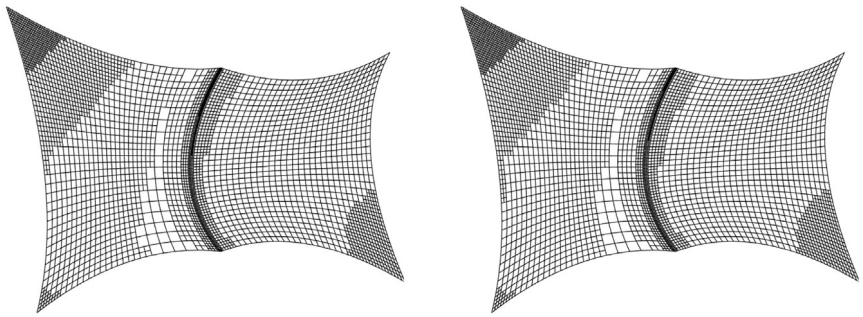

(a) $\mathbf{p} = (3, 3)$, C^0 functions on the interface: NDOF=16310

(b) $\mathbf{p} = (3, 3)$, C^1 functions on the interface: NDOF=15741

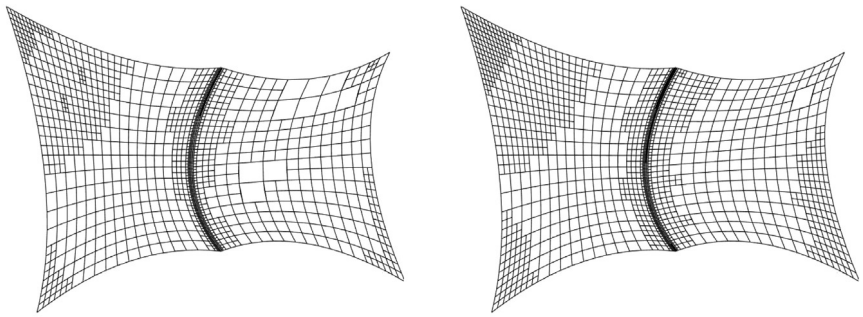

(c) $\mathbf{p} = (4, 4)$, C^0 functions on the interface: NDOF=6357

(d) $\mathbf{p} = (4, 4)$, C^1 functions on the interface: NDOF=7347

Fig. 7. Hierarchical meshes for Example 2, with $\mathbf{p} = (3, 3)$ and $\mathbf{p} = (4, 4)$.

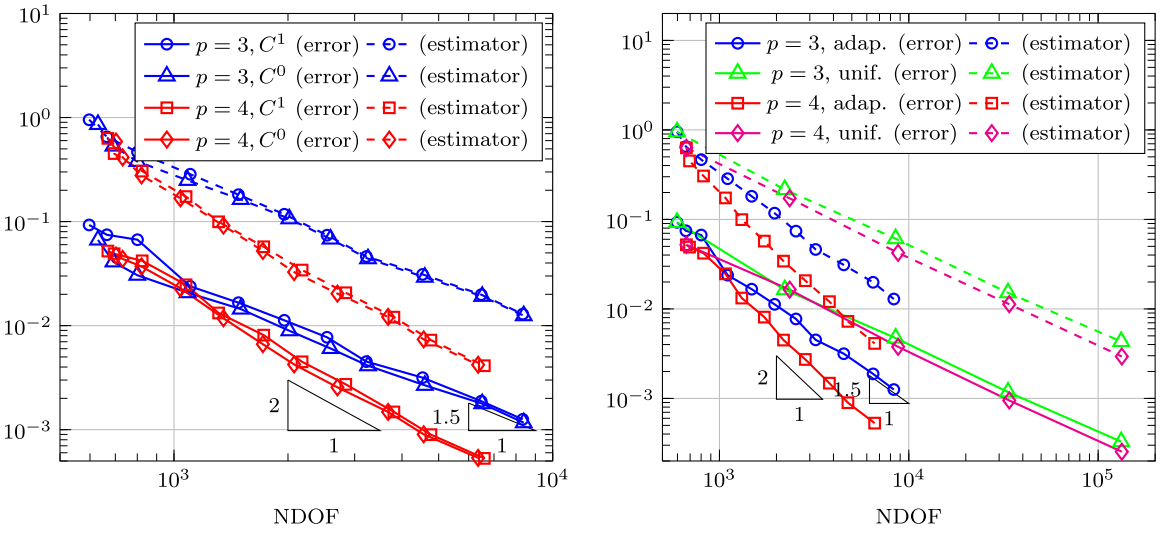

Fig. 8. Error in H^1 semi-norm and estimator for Example 3 with $\mathbf{p} = (3, 3)$ and $\mathbf{p} = (4, 4)$, compared with C^0 case (left) and with global refinement case (right).

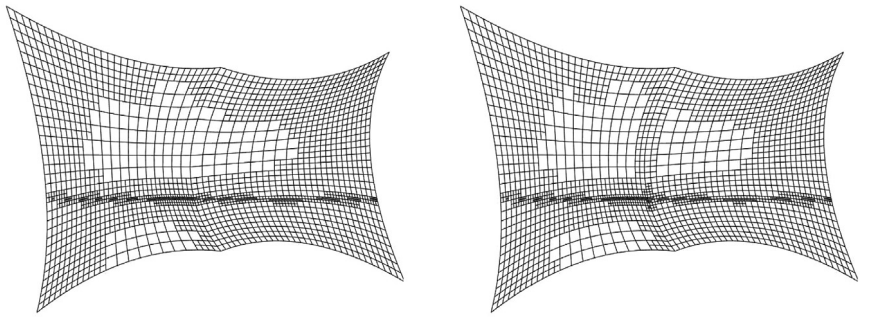

(a) $\mathbf{p} = (3, 3)$, C^0 functions on the interface: NDOF=8388

(b) $\mathbf{p} = (3, 3)$, C^1 functions on the interface: NDOF=8336

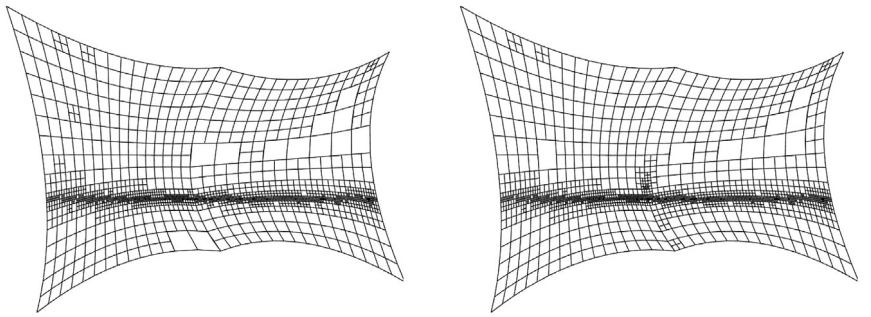

(c) $\mathbf{p} = (4, 4)$, C^0 functions on the interface: NDOF=6356

(d) $\mathbf{p} = (4, 4)$, C^1 functions on the interface: NDOF=6601

Fig. 9. Hierarchical meshes for Example 3, with $\mathbf{p} = (3, 3)$ and $\mathbf{p} = (4, 4)$.

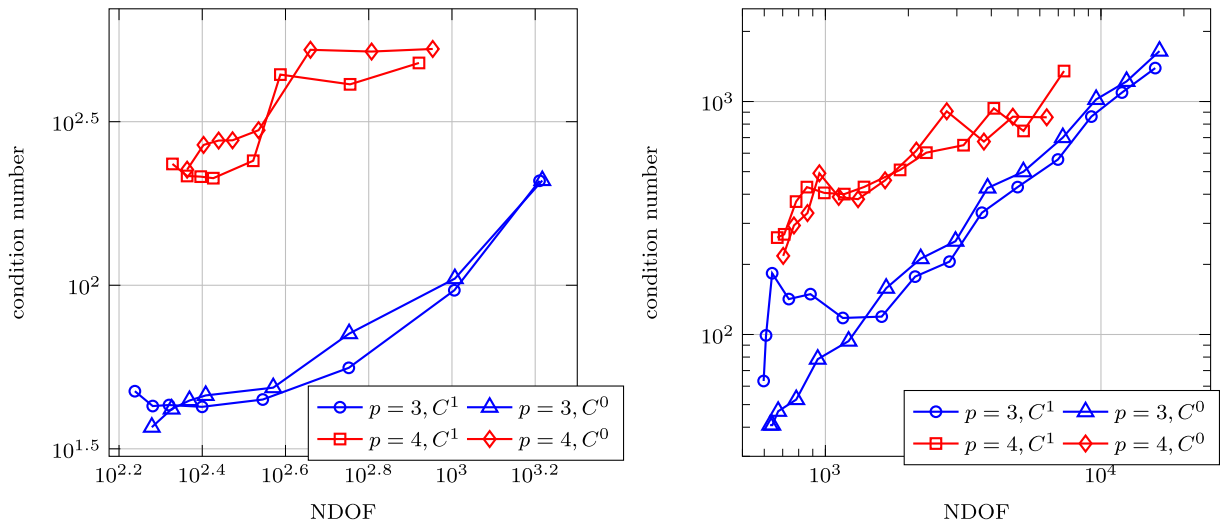

Fig. 10. Comparison of the condition number of the stiffness matrix, after diagonal preconditioning, obtained in the solution of Example 1 (left) and Example 2 (right).

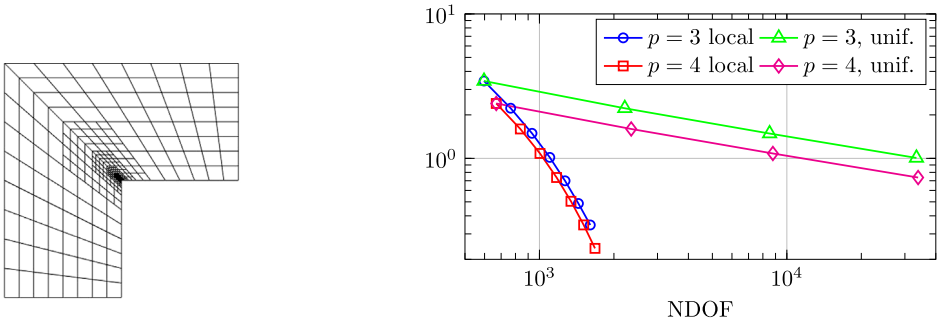

(a) Refinement of the L-shaped domain

(b) Error in H^2 semi-norm

Fig. 11. Hierarchical mesh (a) and comparison of the results obtained by local refinement and C^1 space with global refinement (b) on Example 4.

region surrounding the reentrant corner, and composed of 4×4 elements of the finest level, is marked for refinement, see Fig. 11(a). We remark that the implementation of the adaptive algorithm with a residual-based estimator would require computing fourth order derivatives at the quadrature points, and several jump terms across the interface, that is beyond the scope of the present work.

In Fig. 11(b) we show the error obtained in H^2 semi-norm when computing with C^1 hierarchical splines of degrees 3 and 4 and regularity r equal to degree minus two within the single patches, for the local refinement described above, and with C^1 isogeometric splines of the same degree and inner regularity r with global uniform refinement. It is obvious that the hierarchical spaces perform much better, as we obtain a lower error with many less degrees of freedom. In this case we do not see a big difference between the results obtained for degrees 3 and 4, but this is caused by the fact that we are refining by hand, and the asymptotic regime has not been reached yet.

6. Conclusions

We presented the construction of C^1 hierarchical functions on two-patch geometries and their application in isogeometric analysis. After briefly reviewing the characterization of C^1 tensor-product isogeometric spaces, we investigated the properties needed to effectively use these spaces as background machinery for the hierarchical spline model. In particular, the local linear independence of the one-level basis functions and the nested nature of the considered C^1 splines spaces was proved. We also introduced an explicit expression of the refinement masks under dyadic refinement, that among other things is useful for the practical implementation of the hierarchical basis functions. The numerical examples show that optimal convergence rates are obtained by the local refinement scheme for second and fourth order problems, even

Table A.1
Control points $\widetilde{\mathbf{c}}_{i,j}^{(S)}$, $S \in \{L, R\}$, of the initial non-analysis-suitable G^1 two-patch parameterization $\widetilde{\mathbf{F}}$.

$\widetilde{\mathbf{c}}_{i,j}^{(L)}$			$\widetilde{\mathbf{c}}_{i,j}^{(R)}$		
$(0, 0)$	$(-3, 1/3)$	$(-6, -2)$	$(0, 0)$	$(13/5, 1)$	$(6, -1)$
$(-2, 5/2)$	$(-13/4, 53/20)$	$(-5, 2)$	$(-2, 5/2)$	$(39/20, 3)$	$(4, 11/3)$
$(0, 6)$	$(-3, 17/3)$	$(-7, 8)$	$(0, 6)$	$(3, 5)$	$(11/2, 13/2)$

Table A.2
Control points $\mathbf{c}_{i,j}^{(S)}$, $S \in \{L, R\}$, of the resulting analysis-suitable G^1 two-patch parameterization $\mathbf{F}$.

$\mathbf{c}_{i,j}^{(L)}$			
$(0, 0)$	$(-2, 2/9)$	$(-4, -4/9)$	$(-6, -2)$
$(-4/3, 5/3)$	$(-127/50, 44/25)$	$(-98/25, 37/25)$	$(-16/3, 2/3)$
$(-4/3, 11/3)$	(C_3, C_4)	$(-89/25, 189/50)$	$(-17/3, 4)$
$(0, 6)$	$(-2, 52/9)$	$(-13/3, 58/9)$	$(-7, 8)$
$\mathbf{c}_{i,j}^{(R)}$			
$(0, 0)$	$(26/15, 2/3)$	$(56/15, 1/3)$	$(6, -1)$
$(-4/3, 5/3)$	(C_1, C_2)	$(87/25, 113/50)$	$(14/3, 19/9)$
$(-4/3, 11/3)$	(C_5, C_6)	$(29/10, 4)$	$(9/2, 83/18)$
$(0, 6)$	$(2, 16/3)$	$(23/6, 11/2)$	$(11/2, 13/2)$

in presence of singular solutions. In future work we plan to generalize the construction to the multi-patch domain setting of [45], but this will require a different strategy with respect to the approach presented in this work since the basis functions of a single level may be locally linearly dependent in the neighborhood of extraordinary points. A possible approach is to express the single level basis functions as in the setting of spline manifolds [53], and define different refinement strategies for marked elements depending on the type of chart they belong to.

CRediT authorship contribution statement

Cesare Bracco: Conceptualization, Methodology, Software, Investigation, Writing - original draft, Writing - review & editing, Visualization. **Carlotta Giannelli:** Conceptualization, Methodology, Investigation, Writing - original draft, Writing - review & editing. **Mario Kapl:** Conceptualization, Methodology, Investigation, Writing - original draft, Writing - review & editing. **Rafael Vázquez:** Conceptualization, Methodology, Software, Investigation, Writing - original draft, Writing - review & editing, Visualization.

Acknowledgment

The authors wish to thank the anonymous reviewers for their comments that helped to improve the paper. Cesare Bracco, Carlotta Giannelli and Rafael Vázquez are members of the INdAM Research group GNCS. The INdAM support through GNCS and Finanziamenti Premiali SUNRISE is gratefully acknowledged. Rafael Vázquez has been partially supported by the ERC Advanced Grant "CHANGE", grant number 694515, 2016–2020. Mario Kapl has been partially supported by the Austrian Science Fund (FWF) through the project P 33023.

Appendix. Geometry of the curved domain

The geometry in Fig. 3(b) for the examples in Section 5 is generated by following the algorithm in [39]. This technique is based on solving a quadratic minimization problem with linear side constraints, and constructs from an initial multi-patch geometry $\widetilde{\mathbf{F}}$ an analysis-suitable G^1 multi-patch parameterization $\mathbf{F}$ possessing the same boundary, vertices and first derivatives at the vertices as $\widetilde{\mathbf{F}}$.

In our case, the initial geometry $\widetilde{\mathbf{F}}$ is given by the two patch parameterization consisting of two quadratic Bézier patches $\widetilde{\mathbf{F}}^{(L)}$ and $\widetilde{\mathbf{F}}^{(R)}$ (i.e. without any internal knots) with the control points $\widetilde{\mathbf{c}}_{i,j}^{(S)}$, $S \in \{L, R\}$, specified in Table A.1. This parameterization is not analysis-suitable G^1.

Applying the algorithm in [39] (by using Mathematica), we construct an analysis-suitable G^1 two-patch geometry $\mathbf{F}$ with bicubic Bézier patches $\mathbf{F}^{(L)}$ and $\mathbf{F}^{(R)}$. Their control points $\mathbf{c}_{i,j}^{(S)}$, $S \in \{L, R\}$, are given in Table A.2, where for presenting some of their coordinates the notations $D = 99170$ and

$$C_1 = 333939/D, \qquad C_2 = 47387036/(22.5D),$$
$$C_3 = -15800567/(5D), \qquad C_4 = 242128576/(67.5D),$$
$$C_5 = 57452423/(45D), \qquad C_6 = 81952942/(22.5D),$$

are used.

References

[1] L. Beirão da Veiga, A. Buffa, G. Sangalli, R. Vázquez, Mathematical analysis of variational isogeometric methods, Acta Numer. 23 (2014) 157–287.
[2] J.A. Cottrell, T.J.R. Hughes, Y. Bazilevs, Isogeometric Analysis: Toward Integration of CAD and FEA, John Wiley & Sons, Chichester, England, 2009.
[3] T.J.R. Hughes, J.A. Cottrell, Y. Bazilevs, Isogeometric analysis: CAD, finite elements, NURBS, exact geometry and mesh refinement, Comput. Methods Appl. Mech. Engrg. 194 (39–41) (2005) 4135–4195.
[4] A. Collin, G. Sangalli, T. Takacs, Analysis-suitable G^1 multi-patch parametrizations for C^1 isogeometric spaces, Comput. Aided Geom. Design 47 (2016) 93–113.
[5] M. Kapl, F. Buchegger, M. Bercovier, B. Jüttler, Isogeometric analysis with geometrically continuous functions on planar multi-patch geometries, Comput. Methods Appl. Mech. Engrg. 316 (2017) 209–234.
[6] A. Tagliabue, L. Dedè, A. Quarteroni, Isogeometric analysis and error estimates for high order partial differential equations in fluid dynamics, Comput. Fluids 102 (2014) 277–303.
[7] F. Auricchio, L. Beirão da Veiga, A. Buffa, C. Lovadina, A. Reali, G. Sangalli, A fully locking-free isogeometric approach for plane linear elasticity problems: A stream function formulation, Comput. Methods Appl. Mech. Engrg. 197 (1) (2007) 160–172.
[8] D.J. Benson, Y. Bazilevs, M.-C. Hsu, T.J.R. Hughes, A large deformation, rotation-free, isogeometric shell, Comput. Methods Appl. Mech. Engrg. 200 (13) (2011) 1367–1378.
[9] J. Kiendl, Y. Bazilevs, M.-C. Hsu, R. Wüchner, K.-U. Bletzinger, The bending strip method for isogeometric analysis of Kirchhoff-Love shell structures comprised of multiple patches, Comput. Methods Appl. Mech. Engrg. 199 (35) (2010) 2403–2416.
[10] J. Kiendl, K.-U. Bletzinger, J. Linhard, R. Wüchner, Isogeometric shell analysis with Kirchhoff-Love elements, Comput. Methods Appl. Mech. Engrg. 198 (49) (2009) 3902–3914.
[11] H. Gómez, V.M. Calo, Y. Bazilevs, T.J.R. Hughes, Isogeometric analysis of the Cahn–Hilliard phase-field model, Comput. Methods Appl. Mech. Engrg. 197 (49) (2008) 4333–4352.
[12] H. Gomez, V.M. Calo, T.J.R. Hughes, Isogeometric analysis of Phase–Field models: Application to the Cahn–Hilliard equation, in: ECCOMAS Multidisciplinary Jubilee Symposium: New Computational Challenges in Materials, Structures, and Fluids, Springer, Netherlands, 2009, pp. 1–16.
[13] J. Liu, L. Dedè, J.A. Evans, M.J. Borden, T.J.R. Hughes, Isogeometric analysis of the advective Cahn—Hilliard equation: Spinodal decomposition under shear flow, J. Comput. Phys. 242 (2013) 321–350.
[14] R. Kraft, Adaptive and linearly independent multilevel B–splines, in: A. Le Méhauté, C. Rabut, L.L. Schumaker (Eds.), Surface Fitting and Multiresolution Methods, Vanderbilt University Press, Nashville, 1997, pp. 209–218.
[15] A.-V. Vuong, C. Giannelli, B. Jüttler, B. Simeon, A hierarchical approach to adaptive local refinement in isogeometric analysis, Comput. Methods Appl. Mech. Engrg. 200 (2011) 3554–3567.
[16] C. Giannelli, B. Jüttler, H. Speleers, THB–splines: the truncated basis for hierarchical splines, Comput. Aided Geom. Design 29 (2012) 485–498.
[17] C. Giannelli, B. Jüttler, H. Speleers, Strongly stable bases for adaptively refined multilevel spline spaces, Adv. Comput. Math. 40 (2014) 459–490.
[18] A. Buffa, C. Giannelli, Adaptive isogeometric methods with hierarchical splines: Error estimator and convergence, Math. Models Methods Appl. Sci. 26 (2016) 1–25.
[19] A. Buffa, C. Giannelli, Adaptive isogeometric methods with hierarchical splines: Optimality and convergence rates, Math. Models Methods Appl. Sci. 27 (2017) 2781–2802.
[20] G. Gantner, D. Haberlik, D. Praetorius, Adaptive IGAFEM with optimal convergence rates: Hierarchical B-splines, Math. Models Methods Appl. Sci. 27 (2017) 2631–2674.
[21] D. D'Angella, S. Kollmannsberger, E. Rank, A. Reali, Multi-level Bézier extraction for hierarchical local refinement of Isogeometric Analysis, Comput. Methods Appl. Mech. Engrg. 328 (2018) 147–174.
[22] E. Garau, R. Vázquez, Algorithms for the implementation of adaptive isogeometric methods using hierarchical B-splines, Appl. Numer. Math. 123 (2018) 58–87.
[23] P. Hennig, S. Müller, M. Kästner, Bézier extraction and adaptive refinement of truncated hierarchical NURBS, Comput. Methods Appl. Mech. Engrg. 305 (2016) 316–339.
[24] P. Hennig, M. Ambati, L. De Lorenzis, M. Kästner, Projection and transfer operators in adaptive isogeometric analysis with hierarchical B-splines, Comput. Methods Appl. Mech. Engrg. 334 (2018) 313–336.
[25] G. Lorenzo, M.A. Scott, K. Tew, T.J.R. Hughes, H. Gomez, Hierarchically refined and coarsened splines for moving interface problems, with particular application to phase-field models of prostate tumor growth, Comput. Methods Appl. Mech. Engrg. 319 (2017) 515–548.
[26] J. Hoschek, D. Lasser, Fundamentals of Computer Aided Geometric Design, A K Peters Ltd, Wellesley, MA, 1993.
[27] J. Peters, Geometric continuity, in: Handbook of Computer Aided Geometric Design, North-Holland, Amsterdam, 2002, pp. 193–227.
[28] D. Groisser, J. Peters, Matched G^k-constructions always yield C^k-continuous isogeometric elements, Comput. Aided Geom. Design 34 (2015) 67–72.
[29] F. Buchegger, B. Jüttler, A. Mantzaflaris, Adaptively refined multi-patch B-splines with enhanced smoothness, Appl. Math. Comput. 272 (2016) 159–172.
[30] T. Nguyen, J. Peters, Refinable C^1 spline elements for irregular quad layout, Comput. Aided Geom. Design 43 (2016) 123–130.
[31] D. Toshniwal, H. Speleers, T.J.R. Hughes, Analysis-Suitable Spline Spaces of Arbitrary Degree on Unstructured Quadrilateral Meshes, Technical Report 16, Institute for Computational Engineering and Sciences (ICES), 2017.
[32] D. Toshniwal, H. Speleers, T.J.R. Hughes, Smooth cubic spline spaces on unstructured quadrilateral meshes with particular emphasis on extraordinary points: Geometric design and isogeometric analysis considerations, Comput. Methods Appl. Mech. Engrg. 327 (2017) 411–458.
[33] K. Karčiauskas, T. Nguyen, J. Peters, Generalizing bicubic splines for modeling and IGA with irregular layout, Comput.-Aided Des. 70 (2016) 23–35.
[34] K. Karčiauskas, J. Peters, Refinable bi-quartics for design and analysis, Comput.-Aided Des. (2018) 204–214.
[35] T. Nguyen, K. Karčiauskas, J. Peters, C^1 Finite elements on non-tensor-product 2d and 3d manifolds, Appl. Math. Comput. 272 (2016) 148–158.
[36] U. Reif, A refinable space of smooth spline surfaces of arbitrary topological genus, J. Approx. Theory 90 (2) (1997) 174–199.
[37] T. Nguyen, K. Karčiauskas, J. Peters, A comparative study of several classical, discrete differential and isogeometric methods for solving Poisson's equation on the disk, Axioms 3 (2) (2014) 280–299.
[38] D. Toshniwal, H. Speleers, R. Hiemstra, T.J.R. Hughes, Multi-degree smooth polar splines: A framework for geometric modeling and isogeometric analysis, Comput. Methods Appl. Mech. Engrg. 316 (2017) 1005–1061.
[39] M. Kapl, G. Sangalli, T. Takacs, Construction of analysis-suitable G^1 planar multi-patch parameterizations, Comput.-Aided Des. 97 (2018) 41–55.
[40] M. Bercovier, T. Matskewich, Smooth Bézier Surfaces over Unstructured Quadrilateral Meshes, in: Lecture Notes of the Unione Matematica Italiana, Springer, 2017.
[41] M. Kapl, V. Vitrih, B. Jüttler, K. Birner, Isogeometric analysis with geometrically continuous functions on two-patch geometries, Comput. Math. Appl. 70 (7) (2015) 1518–1538.

[42] A. Blidia, B. Mourrain, N. Villamizar, G^1-smooth splines on quad meshes with 4-split macro-patch elements, Comput. Aided Geom. Design 52–53 (2017) 106–125.
[43] M. Kapl, G. Sangalli, T. Takacs, Dimension and basis construction for analysis-suitable G^1 two-patch parameterizations, Comput. Aided Geom. Design 52–53 (2017) 75–89.
[44] M. Kapl, G. Sangalli, T. Takacs, Isogeometric analysis with C^1 functions on planar, unstructured quadrilateral meshes, SMAI J. Comput. Math. 5 (2019) 67–86.
[45] M. Kapl, G. Sangalli, T. Takacs, An isogeometric C^1 subspace on unstructured multi-patch planar domains, Comput. Aided Geom. Design 69 (2019) 55–75.
[46] B. Mourrain, R. Vidunas, N. Villamizar, Dimension and bases for geometrically continuous splines on surfaces of arbitrary topology, Comput. Aided Geom. Design 45 (2016) 108–133.
[47] C.L. Chan, C. Anitescu, T. Rabczuk, Isogeometric analysis with strong multipatch C^1-coupling, Comput. Aided Geom. Design 62 (2018) 294–310.
[48] C.L. Chan, C. Anitescu, T. Rabczuk, Strong multipatch C^1-coupling for isogeometric analysis on 2D and 3D domains, Comput. Methods Appl. Mech. Engrg. 357 (2019).
[49] R. Vázquez, A new design for the implementation of isogeometric analysis in octave and matlab: GeoPDEs 3.0, Comput. Math. Appl. 72 (2016) 523–554.
[50] C. Bracco, A. Buffa, C. Giannelli, R. Vázquez, Adaptive isogeometric methods with hierarchical splines: an overview, Discrete Contin. Dyn. Syst. 39 (1) (2019).
[51] G. Gantner, Optimal Adaptivity for Splines in Finite and Boundary Element Methods (Ph.D. thesis), Technische Universität Wien, 2017.
[52] P. Grisvard, Singularities in Boundary Value Problems, in: Recherches en Mathématiques Appliquées [Research in Applied Mathematics], vol. 22, Springer-Verlag, Berlin, Masson, Paris, 1992.
[53] G. Sangalli, T. Takacs, R. Vázquez, Unstructured spline spaces for isogeometric analysis based on spline manifolds, Comput. Aided Geom. Design 47 (2016) 61–82.